Molecular and Cellular MR Imaging

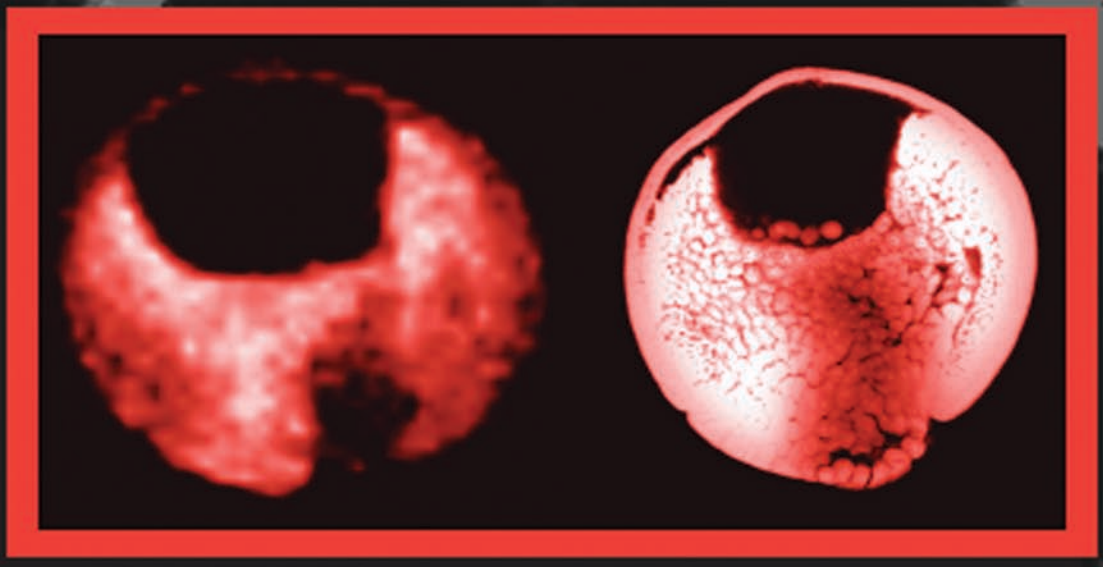

Edited by
Michel M. J. Modo
Jeff W. M. Bulte

CRC Press
Taylor & Francis Group

Molecular and Cellular MR Imaging

Molecular and Cellular MR Imaging

Edited by

Michel M. J. Modo

Jeff W. M. Bulte

CRC Press
Taylor & Francis Group
Boca Raton London New York

CRC Press is an imprint of the
Taylor & Francis Group, an informa business

CRC Press
Taylor & Francis Group
6000 Broken Sound Parkway NW, Suite 300
Boca Raton, FL 33487-2742

Printed in the United States of America on acid-free paper
10 9 8 7 6 5 4 3 2 1

International Standard Book Number-10: 0-8493-7252-6 (Hardcover)
International Standard Book Number-13: 978-0-8493-7252-0 (Hardcover)

Library of Congress Cataloging-in-Publication Data

Molecular and cellular MR imaging / edited by Michel M.J.J. Modo and Jeff W.M. Bulte.
p. ; cm.
Includes bibliographical references and index.
ISBN-13: 978-0-8493-7252-0 (hardcover : alk. paper)
ISBN-10: 0-8493-7252-6 (hardcover : alk. paper)
1. Magnetic resonance imaging. 2. Molecular biology. 3. Cytology. I. Modo, Michel M. J. J. II. Bulte, Jeff W. M.
[DNLM: 1. Magnetic Resonance Imaging--methods. 2. Cytological Techniques--methods. 3. Molecular Diagnostic Techniques--methods. WN 185 M718 2007]

RC78.7.N83M65 2007
616.07'548--dc22 2006035039

Visit the Taylor & Francis Web site at
http://www.taylorandfrancis.com

and the CRC Press Web site at
http://www.crcpress.com

Table of Contents

Chapter 1 What Is Molecular and Cellular Imaging? 1
Michel M.J. Modo and Jeff W.M. Bulte

PART I Contrast Agents for Molecular and Cellular Imaging

Chapter 2 Physicochemical Principles of MR Contrast Agents 13
Peter Caravan

Chapter 3 Paramagnetic Contrast Agents 37
Silvio Aime, Zsolt Baranyai, Eliana Gianolio, and Enzo Terreno

Chapter 4 Superparamagnetic Contrast Agents 59
Claire Corot, Marc Port, Irène Guilbert, Philippe Robert, Isabelle Raynal, Caroline Robic, Jean-Sebastien Raynaud, Philippe Prigent, Anne Dencausse, and Jean-Marc Idée

Chapter 5 Physical Mechanism and Applications of CEST Contrast Agents 85
Michael T. McMahon, Jinyuan Zhou, Assaf A. Gilad, Jeff W.M. Bulte, and Peter C.M. van Zijl

Chapter 6 PARACEST Contrast Agents 101
A. Dean Sherry and Mark Woods

Chapter 7 Genetic Approaches for Modulating MRI Contrast 123
Eric T. Ahrens, William F. Goins, and Clinton S. Robison

PART II Molecular MR Imaging

Chapter 8 Molecular and Functional MR Imaging of Cancer 141
Michael A. Jacobs, Kristine Glunde, Barjor Gimi, Arvind P. Pathak, Ellen Ackerstaff, Dmitri Artemov, and Zaver M. Bhujwalla

Chapter 9 Molecular Imaging of Atherosclerosis with Magnetic Resonance 161
Karen C. Briley-Saebo, Willem J. Mulder, Fabien Hyafil, Venkatesh Mani, Vardan Amirbekian, Juan Gilberto S. Aguinaldo, James F. Rudd, Silvia H. Aguiar, and Zahi A. Fayad

Chapter 10 Molecular Imaging of Apoptosis 183
Mikko I. Kettunen and Kevin M. Brindle

Chapter 11 Molecular Imaging of Reporter Genes 199
Keren Ziv, Dorit Granot, Vicki Plaks, Batya Cohen, and Michal Neeman

Chapter 12 Pharmacological MRI as a Molecular Imaging Technique 219
Y. Iris Chen and Bruce G. Jenkins

PART III Cellular MR Imaging

Chapter 13 Cellular MR Imaging of the Liver Using Contrast Agents 247
N. Cem Balci and Sukru Mehmet Erturk

Chapter 14 Cellular Imaging of Macrophage Activity in Infection and Inflammation 259
Martin Rausch, Markus Rudin, Peter R. Allegrini, and Nicolau Beckmann

Chapter 15 Cellular Imaging of Macrophage Activity in Stroke 273
Ralph Weber and Mathias Hoehn

Chapter 16 Magnetic Resonance Imaging in Developmental Biology 283
Cyrus Papan, J. Michael Tyszka, and Russell E. Jacobs

Chapter 17 Methods for Labeling Nonphagocytic Cells with MR Contrast Agents 295
Joseph A. Frank, Stasia A. Anderson, and Ali S. Arbab

Chapter 18 Cellular Imaging of Cell Transplants 325
Michel M.J. Modo and Jeff W.M. Bulte

Chapter 19 Cellular and Molecular Imaging of the Diabetic Pancreas 343
Zdravka Medarova and Anna Moore

Chapter 20 Functional Cellular Imaging with Manganese 369
Vincent Van Meir and Annemie Van der Linden

PART IV Future Perspectives for Molecular and Cellular Imaging

Chapter 21 Translating Promising Experimental Approaches to Clinical Trials 395
Adrian D. Nunn

Chapter 22 An Outlook on Molecular and Cellular MR Imaging 405
Michel M.J. Modo and Jeff W.M. Bulte

Index 411

Preface

Molecular and cellular magnetic resonance (MR) imaging have recently emerged as novel technologies for the noninvasive assessment of biological processes in living organisms. The possibility to track the survival, migration, and differentiation of cells *in vivo*, as well as to be able to monitor particular gene or protein expression in living subjects, is not only becoming of great interest to scientists investigating fundamental aspects of health and disease, but is now also finding a translation into clinical settings.

The interdisciplinary nature of molecular and cellular MR imaging mandates various backgrounds in molecular and cell biology, chemistry, physics, image analysis, and drug discovery. In this book, a selected group of internationally recognized authors, each drawing on their specific expertise, highlight the diversity of skills necessary to further advance the field of molecular and cellular MR imaging. A constant dialog between these disciplines is vital to develop and translate promising approaches into reliable scientific applications and viable clinical diagnostic tools. This book provides a state-of-the-art overview of the various approaches to date that have been described to visualize cells and molecules by MR imaging and illustrates the application of these to interrogate specific biological processes in both animals and humans.

The Editors

Michel M.J. Modo, Ph.D., a Luxembourg native, is a Research Council of the United Kingdom (RCUK) fellow and Wolfson lecturer in stem cell imaging at the Centre for the Cellular Basis of Behaviour and the Medical Research Council (MRC) Centre for Neurodegeneration Research at the Institute of Psychiatry (IoP), King's College London. Dr. Modo graduated from Royal Holloway University of London with a degree in psychology and in 1995 spent 1 year as an undergraduate in the psychology department at McGill University in Montreal, Canada. In 2001, he earned his Ph.D. at the IoP and has since been interested in the application of molecular and cellular imaging to understand how stem cells promote functional recovery after brain damage.

Jeff W.M. Bulte, M.D., also a native from the Benelux (the Netherlands), is a professor of radiology in the Division of MR Research and is director of the cellular imaging section at the Institute for Cell Engineering, Johns Hopkins University School of Medicine. In 1991, Dr. Bulte graduated summa cum laude in medicine/immunoloy from the University of Groningen, and he spent 10 years in the Laboratory of Diagnostic Radiology Research at the National Institutes of Health before moving to Hopkins in 2001. His research specializes in molecular and cellular MR imaging.

Contributors

Ellen Ackerstaff
Department of Radiology and
Sidney Kimmel Comprehensive Cancer Center
Johns Hopkins University School of Medicine
Baltimore, Maryland

Silvia H. Aguiar
Department of Radiology
Mount Sinai School of Medicine
New York, New York

Juan Gilberto S. Aguinaldo
Department of Radiology
Mount Sinai School of Medicine
New York, New York

Eric T. Ahrens
Carnegie Mellon University
Pittsburgh, Pennsylvania

Silvio Aime
Department of Chemistry
IFM
University of Torino
Torino, Italy

Peter R. Allegrini
Novartis Institute for Biomedical Research
Novartis Pharma AG
Basel, Switzerland

Vardan Amirbekian
Department of Radiology
Mount Sinai School of Medicine
New York, New York

Stasia A. Anderson
National Institutes of Health
Bethesda, Maryland

Ali S. Arbab
Henry Ford Health System
Detroit, Michigan

Dmitri Artemov
Department of Radiology and
Sidney Kimmel Comprehensive Cancer Center
Johns Hopkins University School of Medicine
Baltimore, Maryland

N. Cem Balci
Department of Radiology
Saint Louis University
Saint Louis, Missouri

Zsolt Baranyai
Department of Chemistry
IFM and Molecular Imaging Center
University of Torino
Torino, Italy

Nicolau Beckmann
Novartis Institutes for BioMedical Research
Basel, Switzerland

Zaver M. Bhujwalla
Department of Radiology and
Sidney Kimmel Comprehensive Cancer Center
John Hopkins University School of Medicine
Baltimore, Maryland

Karen C. Briley-Saebo
Department of Radiology
Mount Sinai School of Medicine
New York, New York

Kevin M. Brindle
Department of Biochemistry
University of Cambridge
Cambridge, England

Jeff W.M. Bulte
Institute for Cell Engineering
Johns Hopkins University School of Medicine
Baltimore, Maryland

Peter Caravan
Epix Pharmaceuticals
Cambridge, Massachusetts

Y. Iris Chen
Athinoula A. Martinos Center
Massachusetts General Hospital
Charlestown, Massachusetts

Batya Cohen
Department of Biological Regulation
Weizmann Institute of Science
Rehovot, Israel

Claire Corot
Guerbet Research
Roissy, France

Anne Dencausse
Guerbet Research
Roissy, France

Sukru Mehmet Erturk
Department of Radiology
Brigham and Women's Hospital
Harvard Medical School
Boston, Massachusetts

Zahi A. Fayad
Mount Sinai School of Medicine
New York, New York

Joseph A. Frank
Laboratory of Diagnostic Radiology
Clinical Center
Bethesda, Maryland

Eliana Gianolio
Department of Chemistry
IFM and Molecular Imaging Center
University of Torino
Torino, Italy

Assaf A. Gilad
School of Medicine
Institute of Cell Engineering
Johns Hopkins University School of Medicine
Baltimore, Maryland

Barjor Gimi
Department of Radiology
University of Texas
Southwestern Medical Center
Dallas, Texas

Kristine Glunde
Department of Radiology and
Sidney Kimmel Comprehensive Cancer Center
Johns Hopkins University School of Medicine
Baltimore, Maryland

William F. Goins
Department of Molecular Genetics
School of Medicine
University of Pittsburgh
Pittsburgh, Pennsylvania

Dorit Granot
Department of Biological Regulation
Weizmann Institute of Science
Rehovot, Israel

Irène Guilbert
Guerbet Research
Roissy, France

Mathias Hoehn
Max-Planck-Institute for Neurological Research
Cologne, Germany

Fabien Hyafil
Department of Radiology
Mount Sinai School of Medicine
New York, New York

Jean-Marc Idée
Guerbet Research
Roissy, France

Michael A. Jacobs
Department of Radiology and
Sidney Kimmel Comprehensive Cancer Center
Johns Hopkins University School of Medicine
Baltimore, Maryland

Russell E. Jacobs
Beckman Institute
California Institute of Technology
Pasadena, California

Bruce G. Jenkins
Athinoula A. Martinos Center
Massachusetts General Hospital
Charlestown, Massachusetts

Mikko I. Kettunen
Department of Biochemistry
University of Cambridge
Cambridge, England

Venkatesh Mani
Department of Radiology
Mount Sinai School of Medicine
New York, New York

Michael T. McMahon
Kennedy Krieger Institute
Baltimore, Maryland

Zdravka Medarova
Harvard Medical School
Massachusetts General Hospital
Charlestown, Massachusetts

Michel M.J. Modo
Centre for the Cellular Basis of Behavior
Institute of Psychiatry
King's College London
London, England

Anna Moore
MGM Martinos Center for Biomedical Imaging
Massachusetts General Hospital
Charlestown, Massachusetts

Willem J. Mulder
Biomedical NMR, Department of
Biomedical Engineering
Eindhoven University of Technology
Eindhoven, Netherlands

Michal Neeman
Department of Biological Regulation
Weizmann Institute of Science
Rehovot, Israel

Adrian D. Nunn
Bracco Research USA, Ltd.
Princeton, New Jersey

Cyrus Papan
Institute of Bioengineering and
Nanotechnology
Thenanos, Singapore

Arvind P. Pathak
Department of Radiology and
Sidney Kimmel Comprehensive Cancer Center
Johns Hopkins University School of Medicine
Baltimore, Maryland

Vicki Plaks
Department of Biological Regulation
Weizmann Institute of Science
Rehovot, Israel

Marc Port
Guerbet Research
Roissy, France

Philippe Prigent
Guerbet Research
Roissy, France

Martin Rausch
Novartis Institutes for Biomedical Research,
Analytical and Imaging Science
Basel, Switzerland

Isabelle Raynal
Guerbet Research
Roissy, France

Jean-Sebastien Raynaud
Guerbet Research
Roissy, France

Philippe Robert
Guerbet Research
Roissy, France

Caroline Robic
Guerbet Research
Roissy, France

Clinton S. Robison
Department of Biological Sciences
Carnegie Mellon University
Pittsburgh, Pennsylvania

James F. Rudd
Department of Radiology
Mount Sinai School of Medicine
New York, New York

Markus Rudin
Institute for Biomedical Engineering
ETH and University of Zurich
Zurich, Switzerland

A. Dean Sherry
Department of Chemistry
University of Texas at Dallas
UT-Southwestern Medical Center
Advanced Imaging Research Center
Dallas, Texas

Enzo Terreno
Department of Chemistry
Molecular Imaging Center
University of Torino
Torino, Italy

J. Michael Tyszka
California Institute of Technology
Pasadena, California

Annemie Van der Linden
Bio-Imaging Lab
University of Antwerp
Antwerp, Belgium

Vincent Van Meir
Bio-Imaging Lab
University of Antwerp
Antwerp, Belgium

Peter C.M. van Zijl
F.M. Kirby Center for
Functional Brain Imaging
Kennedy Krieger Institute
Baltimore, Maryland

Ralph Weber
Max-Planck Institute for Neurological Research
and
University Clinic of Essen
Cologne, Germany

Mark Woods
Macrocyclics, Inc.
Dallas, Texas

Jinyuan Zhou
School of Medicine
Institute for Cell Engineering
Johns Hopkins University
Baltimore, Maryland

Keren Ziv
Department of Biological Regulation
Weizmann Institute of Science
Rehovot, Israel

1 What Is Molecular and Cellular Imaging?

Michel M.J. Modo and Jeff W.M. Bulte

CONTENTS

1.1 Introduction 1
1.2 What Is Molecular and Cellular Imaging? 2
1.3 Is There a Need for Molecular and Cellular Imaging in Biomedical Research? 2
1.4 How Does MR Imaging Compare with Other Imaging Modalities? 3
1.5 The Need for MR Contrast Agents 5
References 7

1.1 INTRODUCTION

The development of life is a proficiently orchestrated process of a myriad of distinctive molecules. From DNA to cells and from cells to organs, it is molecules that are the building blocks of all life.[1] Being able to understand how molecules and cells develop into animals also reveals how aberrant molecular or cellular processes contribute to the degeneration of physiological systems. The most powerful medical interventions are therefore deemed to intervene at the earliest stage when a molecular aberration can be detected. It is thought that this "molecular medicine" will not only treat symptoms of disease, but also lead to the prevention of symptoms and stop disease before it can harm the patient.[2,3]

Until recently, the study of these molecules and cells was mainly confined to invasive and irreversible histological and molecular biological techniques. Histological studies utilize a panoply of antibodies that detect highly specific molecules and allow, for instance, the differentiation between a variety of cellular phenotypes. Molecular biological techniques, such as polymerase chain reaction (PCR), can even describe the constituent parts of biological molecules and define "molecular fingerprints" of disease.[4] However, the disadvantage of both techniques is that they cannot easily be used on an intact living specimen. Histological techniques suffer from light scattering, and therefore have a very poor tissue penetration, whereas molecular biological techniques typically require a disintegration of tissue.

Invasive biopsies are needed to pursue these techniques. However, biopsies can cause tissue damage. Consequently, in many circumstances, biopsies are ethically unacceptable as they can result in iatrogenic complications. For instance, molecular changes in the hippocampus that could indicate early pathogenic events in Alzheimer's disease or epilepsy would require deep brain penetration that would injure surrounding tissue. Additionally, the accuracy of biopsies also depends on adequate sampling. If the disease is very localized in a large organ, such as the liver, the biopsy might sample a part of the organ that is not affected by the disease and lead to a false negative. Even if this approach is justified based on peripheral biomarkers, such as increases of a particular protein in the blood, tissue retrieval could only be considered once due to the inflicted damage to the organ. For that reason, biopsies have considerable limitations to present a potential early diagnosis of a disease. It is hence impossible to use this technique to monitor an organ for the

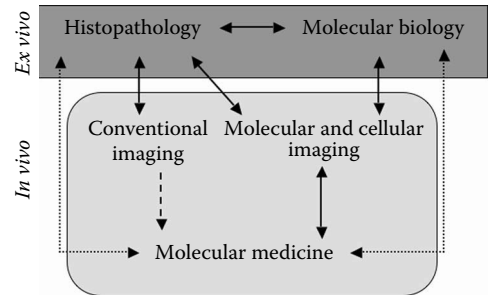

FIGURE 1.1 Both histopathology and molecular biology are predominantly *ex vivo* assessment techniques. In contrast, conventional and molecular and cellular imaging are *in vivo* analytical techniques that can be used to bridge the gap between the need for specific molecular information and its use in patient management in molecular medicine. However, molecular and cellular imaging is very dependent on both histopathology and molecular biology to identify imaging targets. Molecular biology is also dependent on histopathology to identify regions for further molecular analysis, whereas histopathology is dependent on molecular biology to devise probes that allow the localization of particular molecules in tissue sections. The interdependence of different approaches illustrates that particular techniques should not be used in a vacuum, as information derived from another analytical technique will contribute to a faster development. To realize the potential of molecular imaging, these different techniques should complement each other to ensure a rapid progression of technological innovation.

potential emergence of aberrant molecules. These techniques are therefore very limited to study biological or pathological processes in living organisms.

1.2 WHAT IS MOLECULAR AND CELLULAR IMAGING?

The application of histology and molecular biology in humans is very restricted. Neither can provide a satisfactory noninvasive deep tissue visualization of molecules or cells in living organisms. The development of molecular and cellular imaging aims to bridge this gap (Figure 1.1) and provide methods that allow the detection of molecules and their interaction in living organisms over time. To be able to visualize the presence and evolution of molecules or cells noninvasively in an intact animal will form an essential assessment if we are to unravel how life develops and pathology emerges. It is therefore possible to define molecular and cellular imaging as follows:

Molecular imaging — The visualization of specific molecules in an intact animal.
Cellular imaging — The visualization of specific cells in an intact animal.

The visualization of molecules or cells in intact animals distinguishes molecular and cellular imaging from histology and molecular biology that typically require a disintegration of the organisms. The specificity to particular molecules or cells differentiates molecular and cellular imaging from more conventional imaging techniques, such as anatomical and functional magnetic resonance (MR) imaging, which mainly describe gross morphology and organ blood flow. It is thus the target and not necessarily the technique that differentiates molecular or cellular imaging from conventional imaging.

1.3 IS THERE A NEED FOR MOLECULAR AND CELLULAR IMAGING IN BIOMEDICAL RESEARCH?

Although molecular biology might provide the targets for molecular interventions, it is a very poor diagnostic tool, as it lacks application in a living organism and cannot provide deep tissue information

that would allow a spatial localization of an emerging pathogenesis. Over the past few years, it has been highlighted that there is a pressing need for more specific imaging techniques to enhance the *in vivo* study of molecules that are crucial for the development of molecular medicine.[5–7] Because the aim of molecular medicine is to treat molecular aberrations as early as possible, it will be important to develop molecular imaging as a diagnostic tool to allow clinicians to visualize aberrant disease molecules at an early stage in the living subject[8] (Figure 1.1). The realization of molecular medicine is therefore dependent on the development of molecular imaging as a reliable diagnostic tool to provide the bridge between molecular biology and molecular medicine.[5,9]

Apart from its potential application in clinical medicine, molecular and cellular imaging in experimental settings will provide an integrative technology to study biological processes and their relevance to behavior *in vivo*. The integration of behavior, histology, pharmacology, and molecular biology through imaging of these various elements will be essential for a more holistic development of novel approaches. Developments of molecular and cellular imaging will be central to the further development of pharmaceutical and biotechnological research as targets become more and more specific.[6,10] Imaging technology permits researchers to monitor a whole animal to determine effects on multiple organ systems *in vivo*.[11–13] Fine-tuning of pharmacological agents can go beyond current pharmacogenetic matching,[14] by accounting for specific gene expression profiles in particular brain regions. It is foreseeable that this could, for instance, allow the development of pharmacological agents that will target distinct regional neurochemical imbalances in psychiatric disease.

Developments in molecular and cellular imaging will allow the investigation of the elemental constituents of organs, and hence introduce a means to interrogate everything from gene expression to functional circuitries. The ability to link behavior to functional connectivity in the brain and tease out the molecular and anatomical changes underlying the changes through molecular imaging[15] will truly provide a powerful integration of different organizational levels from gene expression to its effect on behavior. As disease-related symptoms are but a modification of normal behavior, it is potentially possible to move beyond symptom-based diagnosis and focus on the specific underlying molecular changes. Although many medical disciplines already base their diagnosis on molecular pathology, this is mainly the case for easily accessible organs, such as the skin, and currently cannot be used for diseases pertaining to the brain or heart. It is therefore likely that medical disciplines concerned with internal organs will have the most to gain from molecular and cellular imaging, and at the same time are likely to see more change in clinical practice than existing approaches.[16] Molecular medicine will not only lead to earlier diagnosis and treatment, but also might redraw the definition of what we consider a disease. However, these predictions and promises are largely dependent on the advances and limits of technological developments in imaging.[9,17–20]

1.4 HOW DOES MR IMAGING COMPARE WITH OTHER IMAGING MODALITIES?

Many different techniques have the capability to visualize molecules *in vivo*.[19] Apart from their physical basis (i.e., the detection of resonant magnetic frequencies, radionuclides, emitted light, etc.), these techniques differ in many other aspects, from their invasiveness to their cost-effectiveness.[6] The choice of the technique will not only be dependent on the molecules or cells one wishes to detect in living subjects, but also be influenced by considering if this approach is to be translated into a clinical setting or if the subject is meant to undergo many repeated assessments. Repeated assessment of invasive procedures complicates clinical translation,[18] but in certain cases some invasiveness might be considered an acceptable risk if it outweighs the information that can be gained in order to help the patient.

Of all the existing molecular imaging techniques, positron emission tomography (PET) and MR imaging are the most advanced and available in both experimental and clinical environments. In contrast to light-dependent techniques, such as bioluminescent imaging, both also have excellent

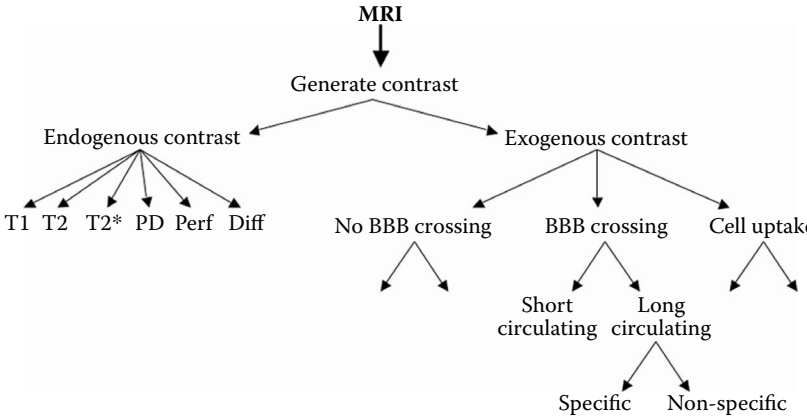

FIGURE 1.2 The basic principle behind MR imaging is to generate contrast between different tissues. Depending on the distribution and movement of water molecules (i.e., hydrogen atoms or protons), different endogenous contrast methods can, for instance, distinguish white from grey matter. However, in some cases exogenously administered contrast can help to highlight particular aspects. For example, the rather large MR contrast agents generally do not cross the intact blood–brain barrier (BBB). Leakage of contrast agents into the brain can therefore be used to assess damage to the BBB. Engineering of contrast agents with peptides that cause an active transport across the blood–brain barrier (e.g., putrescine) can be used to visualize targets that normally cannot be accessed by these agents. Contrast agents can either be cleared rapidly by the body's reticuloendothelial system (RES) or escape detection and generate MR contrast for prolonged episodes. Contrast particles can also either bind to specific targets, such as molecules, or be fairly unspecific and, for instance, merely be used as blood pool agents. Further engineering of MR contrast media will result in ever more sophisticated particles that can cross the intact BBB and be specifically taken up in one particular type of cell.

tissue penetration and, in principle, can visualize a whole subject. PET is a very powerful molecular imaging technique,[21] as the radioligands used to detect particular molecules are minute and easily cross the intact blood–brain barrier. These radioisotopes can easily be attached to other compounds that target particular molecules.[22–25] PET is therefore currently unbeatable in its ability to visualize specific molecules in the living brain.[26,27] However, the dependence on radioisotopes to produce an image in PET is a drawback, as it limits the number of times a single subject can be exposed to this activity.

In contrast, MR imaging mainly relies on detecting the nuclear magnetic resonance (NMR) signal of hydrogen (^{1}H) atoms after the application of a radiofrequency pulse. This noninvasiveness of MR imaging and the lack of radioactivity make it adept for serial studies of the same subject, even with short intervals between imaging sessions. The versatility of MR imaging is also interesting, as there are other MR techniques that complement molecular and cellular MR imaging. Functional/pharmacological MR imaging (f/phMRI), MR spectroscopy (MRS), and interventional MRI (iMRI) are but a few methods that can be achieved with the same hardware that is complementary to molecular/cellular MR imaging. The resolution achieved with MR imaging is largely dependent on the field strength of the magnet as it affects the signal-to-noise ratio (SNR), which determines how well a scan can contrast between different types of tissue (Figure 1.2). The tissue contrast, however, is a function of the distribution and chemical microenvironment of hydrogen atoms (see Chapter 2 for a basic overview of the physics and chemistry of MR imaging). The most commonly used field strengths for clinical scanners are 1.5 and 3.0 tesla (T) (64 and 128 MHz, respectively), whereas experimental studies using animals typically use field strengths at and above 4.7 T (170 MHz), as the target volume is smaller. Depending on the strength of the magnet and the sequences used to scan a subject, different aspects, such as grey or white matter in the brain, can be highlighted.[28]

The high spatial resolution (>10 times higher than PET), excellent tissue contrast, noninvasiveness for serial studies, and versatility make MR imaging a very attractive tool for molecular and cellular imaging that sets it apart from other techniques. Nevertheless, apart from large molecular complexes (e.g., N-acetyl-asparte, choline) that can be detected by MR spectroscopy,[29] MR imaging is not specific to particular molecules or cells. Similar to PET, to achieve specific detection of molecules or cells, MR imaging needs to increase its specificity and sensitivity by means of exogenous tracers or contrast agents.

1.5 THE NEED FOR MR CONTRAST AGENTS

Increasing sensitivity and specificity proves to be the challenge for molecular and cellular MR imaging. The detection of molecular or cellular events needs to exhibit *specificity* for the particular biological event. Specificity is therefore mainly reflected in the high fidelity and reliability of discriminating a particular molecule or cell from noise and other molecules. To achieve this high specificity, an antibody system targeting particular antigen, for instance, will selectively bind to the molecule/cell of interest.[30,31] By combining this antibody with a magnetic contrast agent, it will be possible to provide a selective detection of the molecule or cell of interest with MR imaging. However, other systems exist to specialize MR contrast agents to provide high specificity (Chapters 3 to 7). The properties of the MR contrast agent will determine its binding characteristics to the molecule of interest, its tissue penetration and circulation, and potentially its cellular uptake[32] (Figure 1.2). Modifying MR contrast agents into multifunctional entities (e.g., crossing the blood–brain barrier and selectively detecting amyloid plaques[33]) improves their attractiveness to molecular and cellular imaging.

Based on the functionalization of MR contrast agents, significant advances have been achieved in both cellular and molecular MR imaging (Figure 1.3). Notably, MR contrast agents can be shuttled into different types of cells *in vitro* or *in vivo* to track these by MR imaging[34] (Chapter 18), or they can be engineered to attach to particular molecules on tissues, such as blood vessels.[35] Increasing sophistication in the generation of these particles leads to ever more refined methods to detect specific molecules. For instance, even targeted MR contrast agents will produce a signal change if they are not bound to the molecule of interest. By engineering contrast agents to only produce a signal change when bound to a molecule of interest,[36,37] it is possible to scan the subject sooner, as there is no need to wait for unbound contrast agent to be washed out. These so-called smart MR contrast agents are but the start of contrast agents that change their properties depending on the environment[38] (Chapter 7). Environment sensing agents can be used for MR measurements as diverse as pH,[39] temperature,[40] or molecular interactions.[41] In the context of genetic studies, environmentally influenced agents can be biologically regulated to reflect an upregulation of a gene. Notably, the gene responsible for ferritin transport into cells can be used as an MR reporter[42] by increasing the intracellular iron load that can be detected by T_2*-weighted sequences (Chapters 7 and 11). As the molecular targets for visualization get sparser and more sophisticated, a greater emphasis needs to be placed on being able to detect fewer molecules in a smaller space.

The hardware systems used for visualization of a specific biological event hence need to achieve sufficient *sensitivity* to detect the effect of these MR "reporters." Although increasing the field strength of the MR scanner can improve some of these detection issues, the different physical characteristics of metal particles can facilitate the detection of sparse elements even within a relatively low magnetic field. Of the most commonly used MR contrast agents (gadolinium, ferric iron, and manganese), only iron particles are ferrimagnetic and produce a blooming effect that involves an area substantially greater than its localization.[43–45] Even small quantities of iron oxide particles can therefore be detected on MR scans. In some cases, even a single particle or cell can be detected.[46–48] In other cases, however, iron oxide particles might not be desirable, as the molecule might be too widely distributed throughout the organ and the use of ferumoxides might create a large signal void that no longer allows the localization of these events. Contrast agents based on

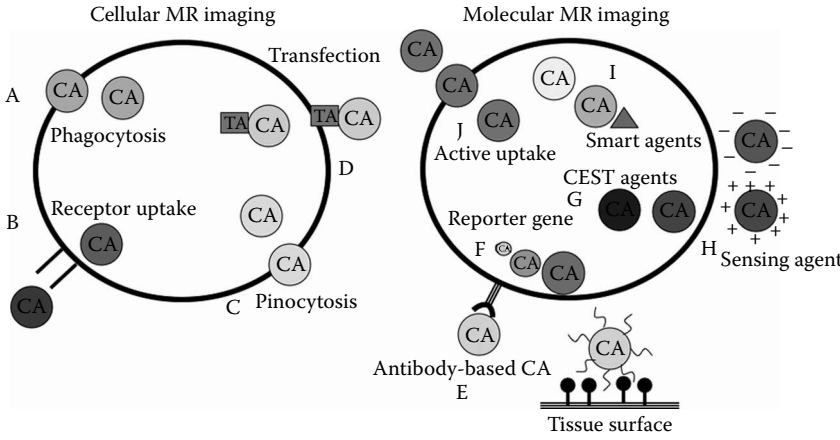

FIGURE 1.3 (please see color insert following page 210) Schematic overview of different approaches used to detect cells or molecules by MR imaging. For cellular imaging, contrast agent can be taken up by cells through phagocytosis (A), receptors (B), or pinocytosis (C). However, generally cells do not readily take up large compounds, but coating of particles with transfection agent can significantly improve uptake into cells (D). Specific molecules can be detected by MR imaging by conjugating an antibody with the contrast particle (E). Although antibodies generally recognize antigens, such as proteins, which are downstream products of a gene, it is also possible to directly study gene expression by genetically engineered cells to express ferritin that leads to a cellular increase in iron that can be detected by MR imaging (F). This reporter gene can then be linked to any gene of interest to study its expression *in vitro* or *in vivo*. Changes in the cell or tissue environment can also be detected by means of contrast agents. Chemical exchange saturation transfer (CEST) agents can be selectively activated by very narrow radiofrequency bands (G), whereas sensing agents change their relaxivity depending on the environmental conditions they encounter (H). However, sensing agents typically have a residual relaxivity, whereas smart agents will only induce a change in MR relaxivity when they bind to a particular molecule (I). Some contrast agents, such as manganese, can also be used to study, for instance, Ca^{2+} uptake into cells, as it normally enters through the Ca^{2+} channel when cells are activated (J).

gadolinium or manganese, producing hyperintensities in T_1-weighted images, might serve as alternatives in these cases. Contrast agents producing hyperintense signals are generally preferable to compounds causing hypointensities, as a positive signal is easier to interpret than the loss of a signal. Nevertheless, T_1 agents also often induce hypointensities on T_2-weighted scans, and therefore might not entirely circumvent this issue. Ideally, contrast agents use alternative atoms, such as fluorine,[49,50] to allow the detection of the molecular target or cell in a scan that does not affect the anatomical hydrogen-based MR image. At present, however, in most experiments iron oxide particles are the preferred agents, as they provide sufficient relaxivity to reliably detect even minute concentrations of contrast agent. Engineering of contrast agents based on their physicochemical properties therefore greatly influences *in vivo* MR detection. Meticulous considerations to these characteristics will ensure significant improvements in the application of molecular imaging agents.[45]

Although contrast agent design and engineering are developing rapidly and progressing the frontiers of molecular imaging, one of the greatest challenges over the coming years will be to ensure that these exciting advances find their translation into clinical applications. Not only will preclinical studies need to determine the feasibility and reliability of these novel contrast agents, but also prior to implementation in human subjects the safety of the newly engineered agents will need to be evaluated[32] (Chapter 21 deals with the clinical implementation of molecular and cellular MR agents). MR contrast agents so far have an excellent record of safety;[51] care must be taken to ensure that the procedures for translation of molecular and cellular imaging follow similar stringent tests and analyses that vouch for the agents' biocompatibility. The use of contrast agents to visualize intracellular targets or the use of contrast agents for cellular MR imaging especially needs to be

thoroughly assessed, as they will remain localized to the compartments for considerably longer time frames than agents that are used for current conventional MR imaging.[34] The further engineering and addition of particular molecules to MR contrast agent demand also further refinement to biocompatibility testing. For instance, immunogenecity of peptides targeting particular molecules might arise as an issue. To date, only a few examples of dextran allergies prevent the use of contrast agents in humans.[52–54] However, as more specific elements enter contrast agent development, more of these compounds might elicit an immune response. Often these particular effects cannot be thoroughly assessed in preclinical experiments. In the future, the extensive testing for biocompatibility in human subjects might become a more complex procedure for the implementation of novel compounds prior to the testing of their specificity for particular molecules. Although many of these issues to date are mainly theoretical considerations, as clinical translations progress, the methods will find further refinement and improve the use of these agents.

There is no question that considerable progress has been achieved in MR contrast agent design. The improved specificity of these compounds and their more targeted application increase the potential of MR imaging as an analytical platform. The possibility to develop MR imaging methods in preclinical models and easily translate this approach to clinical application is central to this rapid progress. The versatility of MR imaging, its complementarities, and integration with other techniques, such as PET and single photon emission computer tomography (SPECT),[55,56] further enhance the attractiveness of MR imaging as a core integrative technique for cellular and molecular imaging. The development of multimodal agents further promises to expand the utility and versatility of MR imaging.[57]

Molecular and cellular MR imaging are interdisciplinary fields of study that require highly specialized expertise in contrast agent chemistry, MR physics, image analysis, and biological disciplines. It is this successful collaboration between different specialties that will progress MR imaging into a molecular and cellular imaging tool central to diagnostic analyses required for molecular medicine to flourish. This book aims to provide an integrated overview of these emerging fields.

REFERENCES

1. Gawad, C., Towards molecular medicine: a case for a biological periodic table, *Am. J. Pharmacogenomics*, 5, 207–211, 2005.
2. Dietel, M. and Sers, C., Personalized medicine and development of targeted therapies: the upcoming challenge for diagnostic molecular pathology. A review, *Virchows Arch.*, 448(6), 744–755, 2006.
3. Steel, M., Molecular medicine: promises, promises? *J. R. Soc. Med.*, 98, 197–199, 2005.
4. Bailey, W.J. and Ulrich, R., Molecular profiling approaches for identifying novel biomarkers, *Expert Opin. Drug Saf.*, 3, 137–151, 2004.
5. Heckl, S., Pipkorn, R., Nagele, T., Vogel, U., Kuker, W., and Voight, K., Molecular imaging: bridging the gap between neuroradiology and neurohistology, *Histol. Histopathol.*, 19, 651–668, 2004.
6. Rudin, M. and Weissleder, R., Molecular imaging in drug discovery and development, *Nat. Rev. Drug Discov.*, 2, 123–131, 2003.
7. Weissleder, R., Molecular imaging: exploring the next frontier, *Radiology*, 212, 609–614, 1999.
8. Calvo, B.F. and Semelka, R.C., Beyond anatomy: MR imaging as a molecular diagnostic tool, *Surg. Oncol. Clin. N. Am.*, 8, 171–183, 1999.
9. Schwaiger, M. and Weber, W., Molecular imaging: dream or reality? *Ernst Schering Res. Found. Workshop*, 48, 1–18, 2004.
10. Herschman, H.R., Molecular imaging: looking at problems, seeing solutions, *Science*, 302, 605–608, 2003.
11. Piwnica-Worms, D., Schuster, D.P., and Garbow, J.R., Molecular imaging of host-pathogen interactions in intact small animals, *Cell. Microbiol.*, 6, 319–331, 2004.
12. Gheysens, O. and Gambhir, S.S., Studying molecular and cellular processes in the intact organism, *Prog. Drug Res.*, 62, 117–150, 2005.

13. Massoud, T.F. and Gambhir, S.S., Molecular imaging in living subjects: seeing fundamental biological processes in a new light, *Genes Dev.*, 17, 545–580, 2003.
14. Staddon, S., Arranz, M.J., Mancama, D., Mata, I., and Kerwin, R.W., Clinical applications of pharmacogenetics in psychiatry, *Psychopharmacology (Berl.)*, 162, 18–23, 2002.
15. Jasanoff, A., Functional MRI using molecular imaging agents, *Trends Neurosci*., 28, 120–126, 2005.
16. Ryan, J.M., Loy, R., and Tariot, P.N., Impact of molecular medicine on neuropsychiatry: the clinician's perspective, *Curr. Psychiatry Rep*., 3, 355–360, 2001.
17. Jager, P.L., de Korte, M.A., Lub-de Hooge, M.N., van Waarde, A., Koopmans, K.P., Perik, P.J., and de Vries, E.G., Molecular imaging: what can be used today, *Cancer Imaging*, 5, S27–S32, 2005.
18. Pomper, M.G., Translational molecular imaging for cancer, *Cancer Imaging*, 5, S16–S26, 2005.
19. Levin, C.S., Primer on molecular imaging technology, *Eur. J. Nucl. Med. Mol. Imaging*, 32 (Suppl. 2), S325–S345, 2005.
20. Frost, J.J., Molecular imaging of the brain: a historical perspective, *Neuroimaging Clin. N. Am*., 13, 653–658, 2003.
21. Hoh, C.K., Schiepers, C., Seltzer, M.A., Gambhir, S.S., Silverman, D.H., Czernin, J., Maddahi, J., and Phelps, M.E., PET in oncology: will it replace the other modalities? *Semin. Nucl. Med*., 27, 94–106, 1997.
22. Conti, P.S., Introduction to imaging brain tumor metabolism with positron emission tomography (PET), *Cancer Invest*., 13, 244–259, 1995.
23. Gibson, R.E., Burns, H.D., Hamill, T.G., Eng, W.S., Francis, B.E., and Ryan, C., Non-invasive radiotracer imaging as a tool for drug development, *Curr. Pharm. Design*, 6, 973–989, 2000.
24. Halldin, C., Gulyas, B., Langer, O., and Farde, L., Brain radioligands: state of the art and new trends, *Q. J. Nucl. Med*., 45, 139–152, 2001.
25. Kegeles, L.S. and Mann, J.J., *In vivo* imaging of neurotransmitter systems using radiolabeled receptor ligands, *Neuropsychopharmacology*, 17, 293–307, 1997.
26. Phelps, M.E., PET: the merging of biology and imaging into molecular imaging, *J. Nucl. Med*., 41, 661–681, 2000.
27. Czernin, J. and Phelps, M.E., Positron emission tomography scanning: current and future applications, *Annu. Rev. Med*., 53, 89–112, 2002.
28. Sasaki, M., Inoue, T., Tohyama, K., Oikawa, H., Ehara, S., and Ogawa, A., High-field MRI of the central nervous system: current approaches to clinical and microscopic imaging, *Magn. Reson. Med. Sci*., 2, 133–139, 2003.
29. Kwock, L., Localized MR spectroscopy: basic principles, *Neuroimaging Clin. N. Am*., 8, 713–731, 1998.
30. Guccione, S., Li, K.C., and Bednarski, M.D., Molecular imaging and therapy directed at the neovasculature in pathologies. How imaging can be incorporated into vascular-targeted delivery systems to generate active therapeutic agents, *IEEE Eng. Med. Biol. Mag*., 23, 50–56, 2004.
31. Artemov, D., Molecular magnetic resonance imaging with targeted contrast agents, *J. Cell. Biochem*., 90, 518–524, 2003.
32. Lorusso, V., Pascolo, L., Fernetti, C., Anelli, P.L., Uggeri, F., and Tiribelli, C., Magnetic resonance contrast agents: from the bench to the patient, *Curr. Pharm. Design*, 11, 4079–4098, 2005.
33. Podulso, J.F., Wengenack, T.M., Curran, G.L., Wisniewski, T., Sigurdsson, E.M., Macura, S.I., Borowski, B.J., and Jack, C.R., Molecular targeting of Alzheimer's amyloid plaques for contrast-enhanced magnetic resonance imaging, *Neurobiol. Dis*., 11, 315–329, 2002.
34. Modo, M., Hoehn, M., and Bulte, J.W., Cellular MR imaging, *Mol. Imaging*, 4, 143–164, 2005.
35. Delikatny, E.J. and Poptani, H., MR techniques for *in vivo* molecular and cellular imaging, *Radiol. Clin. N. Am*., 43, 205–220, 2005.
36. Louie, A.Y., Huber, M.M., Ahrens, E.T., Rothbacher, U., Moats, R., Jacobs, R.E., Fraser, S.E., and Meade, T.J., *In vivo* visualization of gene expression using magnetic resonance imaging, *Nat. Biotechnol*., 18, 321–325, 2000.
37. Li, W.H., Parigi, G., Fragai, M., Luchinat, C., and Meade, T.J., Mechanistic studies of a calcium-dependent MRI contrast agent, *Inorg. Chem*., 41, 4018–4024, 2002.
38. Lowe, M.P., Activated MR contrast agents, *Curr. Pharm. Biotechnol*., 5, 519–528, 2004.
39. Aime, S., Delli Castelli, D., and Terreno, E., Novel pH-reporter MRI contrast agents, *Angew. Chem. Int. Ed. Engl*., 41, 4334–4336, 2002.

40. Aime, S., Botta, M., Fasano, M., Terreno, E., Kinchesh, P., Calabi, L., and Paleari, L., A new ytterbium chelate as contrast agent in chemical shift imaging and temperature sensitive probe for MR spectroscopy, *Magn. Reson. Med.*, 35, 648–651, 1996.
41. Perez, J.M., Josephson, L., O'Loughlin, T., Hogemann, D., and Weissleder, R., Magnetic relaxation switches capable of sensing molecular interactions, *Nat. Biotechnol.*, 20, 816–820, 2002.
42. Cohen, B., Dafni, H., Meir, G., and Neeman, M., Ferritin as novel MR-reporter for molecular imaging of gene expression, *Proc. Int. Soc. Magn. Reson. Med.*, 11, 1707, 2004.
43. Bonnemain, B., Superparamagnetic agents in magnetic resonance imaging: physicochemical characteristics and clinical applications. A review, *J. Drug Target*, 6, 167–174, 1998.
44. Bjornerud, A. and Johansson, L., The utility of superparamagnetic contrast agents in MRI: theoretical consideration and applications in the cardiovascular system, *NMR Biomed.*, 17, 465–477, 2004.
45. Reichert, D.E., Lewis, J.S., and Anderson, C.J., Metal complexes as diagnostic tools, *Coordination Chem. Rev.*, 184, 3–66, 1999.
46. Shapiro, E.M., Sharer, K., Skrtic, S., and Koretsky, A.P., *In vivo* detection of single cells by MRI, *Magn. Reson. Med.*, 55, 242–249, 2006.
47. Heyn, C., Ronald, J.A., Mackenzie, L.T., MacDonald, I.C., Chambers, A.F., Rutt, B.K., and Foster, P.J., *In vivo* magnetic resonance imaging of single cells in mouse brain with optical validation, *Magn. Reson. Med.*, 55, 23–29, 2006.
48. Shapiro, E.M., Skrtic, S., Sharer, K., Hill, J.M., Dunbar, C.E., and Koretsky, A.P., MRI detection of single particles for cellular imaging, *Proc. Natl. Acad. Sci. U.S.A.*, 101, 10901–10906, 2004.
49. Ahrens, E.T., Flores, R., Xu, H., and Morel, P.A., *In vivo* imaging platform for tracking immunotherapeutic cells, *Nat. Biotechnol.*, 23, 983–987, 2005.
50. Schwarz, R., Schuurmans, M., Seelig, J., and Kunnecke, B., 19F-MRI of perfluorononane as a novel contrast modality for gastrointestinal imaging, *Magn. Reson. Med.*, 41, 80–86, 1999.
51. Runge, V.M., Safety of approved MR contrast media for intravenous injection, *J. Magn. Reson. Imaging*, 12, 205–213, 2000.
52. Li, A., Wong, C.S., Wong, M.K., Lee, C.M., and Au Yeung, M.C., Acute adverse reactions to magnetic resonance contrast media: gadolinium chelates, *Br. J. Radiol.*, 79, 368–371, 2006.
53. Beaudouin, E., Kanny, G., Blanloeil, Y., Guilloux, L., Renaudin, J.M., and Moneret-Vautrin, D.A., Anaphylactic shock induced by gadoterate meglumine (DOTAREM), *Allerg. Immunol. (Paris)*, 35, 382–385, 2003.
54. Chu, W.C., Lam, W.W., and Metreweli, C., Incidence of adverse events after I.V. injection of MR contrast agents in a Chinese population. A comparison between gadopentetate and gadodiamide, *Acta Radiol.*, 41, 662–666, 2000.
55. Marsden, P.K., Strul, D., Keevil, S.F., Williams, S.C., and Cash, D., Simultaneous PET and NMR, *Br. J. Radiol.*, 75, S53–S59, 2002.
56. Jacobs, R.E. and Cherry, S.R., Complementary emerging techniques: high-resolution PET and MRI, *Curr. Opin. Neurobiol.*, 11, 621–629, 2001.
57. Roberts, T.P., Chuang, N., and Roberts, H.C., Neuroimaging: do we really need new contrast agents for MRI? *Eur. J. Radiol.*, 34, 166–178, 2000.

Part I

Contrast Agents for Molecular and Cellular Imaging

2 Physicochemical Principles of MR Contrast Agents

Peter Caravan

CONTENTS

2.1 Introduction 13
2.2 A Few Basic Principles of NMR 14
2.3 T_1, T_2, and T_2* Contrast Agents and Relaxivity 15
2.4 Chemistry of T_1 Agents 16
2.5 Paramagnetic Enhanced Nuclear Relaxation 17
2.6 T2 Agents 23
2.7 Imaging Physics: T_1 and T_2 Agents 25
2.8 PARACEST Agents 28
2.9 Direct Observation of Nonhydrogen Nuclei 31
2.10 Common Features and Concerns 32
2.11 Conclusion 32
References 33

2.1 INTRODUCTION

The magnetic resonance (MR) image in clinical and biological systems is typically an image of the hydrogen atoms in water and fat. Water hydrogen is chosen because it is very abundant; tissue is about 90 *M* (molar) in water hydrogen concentration. The ^{1}H isotope (the proton) is almost 100% naturally abundant and is the second most sensitive nucleus, behind tritium, ^{3}H, for nuclear magnetic resonance (NMR) detection. There are many sources of contrast in an MR image. The simplest is proton density, where tissue containing more water will give a greater signal. Tissue contrast can also be achieved by weighting the imaging sequence to display differences in proton relaxation rates ($1/T_1$ and $1/T_2$); exploiting differences in chemical shift or water diffusion; or the effect of flowing blood; or using magnetization transfer techniques. By utilizing one or more of these techniques, high-resolution images can be obtained providing excellent anatomical content, delineation of diseased tissue, and often valuable physiological information.

Sometimes additional contrast is required and exogenous materials are given that can alter the MR signal. These materials are called contrast agents. Contrast agents can act by changing the relaxation rates of neighboring water molecules and giving positive or negative contrast on a T_1- or T_2-weighted imaging sequence, respectively. A different class of contrast agent relies on magnetization transfer to provide negative contrast. Magnetization transfer and T_1- and T_2-weighted agents alter some property of water in a catalytic way, but it is still the water that is imaged. Other contrast agents use alternative nuclei such as fluorine or hyperpolarized nuclei such as carbon, helium, or xenon, and these nuclei are imaged directly.

There is an active research effort to extend MR imaging (MRI) beyond anatomy and physiology to the cellular and molecular level. Contrast agents are used to provide this information. The aim

of this chapter is to provide an overview of the different contrast mechanisms and the relevant chemistry and biophysics for each class of contrast agent. Issues common to all contrast agents, such as formulation, speciation, stability, targeting, and excretion, are also discussed. Each specific class of contrast agent and its application to molecular and cellular imaging are described in greater detail in subsequent chapters in this book. This chapter assumes the reader has a basic knowledge of MRI and its terminology. Textbooks on the basic principles of MRI should be consulted for more detail than is given here.[1,2]

2.2 A FEW BASIC PRINCIPLES OF NMR

Atomic nuclei have magnetic moments that are proportional to their nuclear spin, I. The hydrogen atom has a spin of $^1/_2$. When an external magnetic field is applied, the nuclear moments align themselves with only certain allowed orientations; for $I = {}^1/_2$, there are only two possible orientations, denoted by the magnetic quantum number m_I, which has values of $+{}^1/_2$ or $-{}^1/_2$. In the case of hydrogen, the spins align either with or against the applied magnetic field. The spins can transition between these two states if the appropriate resonant energy (ΔE) is applied:

$$\Delta E = h\nu = \frac{\gamma h B_0}{2\pi} \tag{2.1}$$

Here γ is the magnetogyric ratio, a property specific to the nucleus in question, ν is the applied frequency (sometimes called Larmor frequency), B_0 is the external applied field, and h is Planck's constant. The frequency required will depend directly on the applied field and the magnetogyric ratio. If there is a difference in the population of spins between the $+{}^1/_2$ and $-{}^1/_2$ states, there will be a net absorption of energy when frequency ν is applied. The ratio of the population ($N_{-1/2}/N_{+1/2}$) between these two states is given by the Boltzmann equation:

$$\begin{aligned} \frac{N_{-1/2}}{N_{+1/2}} &= \exp(-h\nu / kT) \\ &= 1 - h\nu / kT; \qquad \text{since } h\nu << kT \end{aligned} \tag{2.2}$$

Since NMR deals with frequencies in the megahertz range, the excess population of spins is only about 1 in 100,000. This is the fundamental reason for the low sensitivity of NMR — only 0.001% of the hydrogen is detected.

Consideration of Equations 2.1 and 2.2 suggests that to increase sensitivity, one should work with a nucleus of high γ and at high applied fields, since this results in the greatest frequency required. Frequency is directly proportional to sensitivity. This is why hydrogen is often used (second highest γ of all nuclei) and why there is a push to higher-field MR imagers. Water is typically imaged because it is the most concentrated of all hydrogen-containing molecules. Fluorine also has a high γ, and highly concentrated perfluoro compounds have been imaged directly. Sensitivity could also be increased if the ratio in Equation 2.2 could be made much smaller. For certain nuclei (^{13}C, ^{129}Xe, ^{3}He), it is possible to polarize the material at low temperature, where kT is small, and then warm the material to room temperature and yet maintain this hyperpolarization.

When nuclei are placed in a magnetic field, it takes a certain time for them to align with or against the field. The time constant for this rate of alignment is called T_1. When radiofrequency (rf) is applied, spins absorb energy and undergo transitions between the $+{}^1/_2$ and $-{}^1/_2$ states. After the radiofrequency pulse is switched off, the spins emit energy and return to their initial equilibrium state. It is this emission of energy that is detected in the imaging experiment. The rate at which the nuclei return to their initial state is termed relaxation: for the component of magnetization

parallel to the external field, the time constant is T_1, the longitudinal (also called spin-lattice) relaxation time; for the component of magnetization perpendicular to the external field, the time constant is T_2, the transverse (also called spin-spin) relaxation time. Transverse relaxation occurs because of local magnetic field inhomogeneities that are caused by (1) microscopic effects caused by magnetic interactions between neighboring molecules (chemistry) and (2) macroscopic effects related to the spatial variation of the external field (physics), e.g., through differences in magnetic susceptibility between air and liquid. The aggregate effect is termed T_2*, while relaxation just due to molecular effects is termed T_2. Although typically it is only water that is detected, water in different tissues has different relaxation times. By making the image acquisition sensitive to differences in T_1, T_2, and T_2*, contrast can be generated.

2.3 T_1, T_2, AND T_2* CONTRAST AGENTS AND RELAXIVITY

In a T_1-weighted image, the repetition time (TR) is set short relative to T_1. Under these conditions, water hydrogens with long T_1 are not given enough time to relax (emit energy) before the next pulse of radiofrequency energy, and so the signal detected from these hydrogens is low. If T_1 is short, then relaxation is fast and most of the signal can be detected. Short T_1 results in positive image contrast.

In a T_2-weighted image, the echo repetition time (TE) is long relative to T_2. Here, fast transverse relaxation leads to signal loss. In a T_2-weighted image, tissue with long T_2 gives positive contrast, while regions with short T_2 will appear dark. Similarly, in T_2*-weighted images (typically gradient echo images), tissue with short T_2* will appear dark.

All contrast agents shorten T_1, T_2, and T_2*. However, it is useful to classify MRI contrast agents into two broad groups based on whether the substance increases the transverse relaxation rate ($1/T_2$) by roughly the same amount that it increases the longitudinal relaxation rate ($1/T_1$) or whether $1/T_2$ is altered to a much greater extent. The first category is referred to as T_1 agents because, on a percentage basis, these agents alter $1/T_1$ of tissue more than $1/T_2$, owing to the fast endogenous transverse relaxation in tissue. With most pulse sequences, this dominant T_1 lowering effect gives rise to increases in signal intensity; these are positive contrast agents. The T_2 agents largely increase the $1/T_2$ of tissue selectively and cause a reduction in signal intensity; these are negative contrast agents. Paramagnetic gadolinium- and manganese-based contrast agents are examples of T_1 agents, while ferromagnetic and superparamagnetic iron oxide particles are examples of T_2 agents.

There are many mechanisms by which contrast agents shorten T_1 and T_2, but in many cases the effect of these mechanisms can be reduced to a single constant, called relaxivity. The simple way to quantify this effect is to consider the rate of relaxation, $1/T_1$ (sometimes denoted R_1). For most cases in medical imaging, the contrast agent increases the relaxation rate proportional to the amount of contrast agent:

$$\frac{1}{T_1} = \frac{1}{T_{1o}} + r_1\,[\mathrm{CA}] \tag{2.3}$$

where T_1 is the observed T_1 with contrast agent in the tissue, T_{1o} is the T_1 prior to addition of the contrast agent, [CA] is the concentration of contrast agent, and r_1 is the longitudinal relaxivity, often just relaxivity. The conventional units for r_1 are $mM^{-1}sec^{-1}$ (per millimolar per second, sometimes written as $l{\cdot}mol^{-1}sec^{-1}$). Thus, the slope of $1/T_1$ as a function of contrast agent concentration reveals the relaxivity. Transverse, or T_2, relaxivity is defined in an analogous way:

$$\frac{1}{T_2} = \frac{1}{T_{2o}} + r_2\,[\mathrm{CA}] \tag{2.4}$$

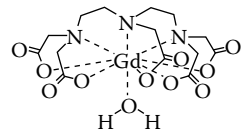

Gd-DTPA (Magnevist®)
Gadopenetate

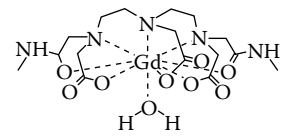

Gd-DTPA-BMA (Omniscan®)
Gadodiamide

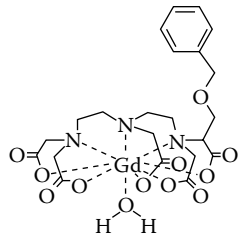

Gd-BOPTA (MultiHance®)
Gadobenate

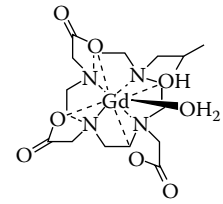

Gd-HPDO3A (ProHance®)
Gadoteridol

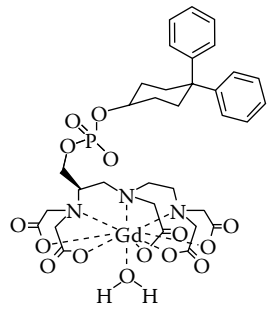

MS-325 (Vasovist®)
Gadofosveset

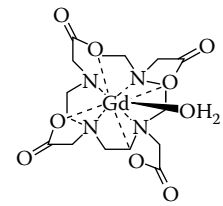

Gd-DOTA (Dotarem®)
Gadoterate

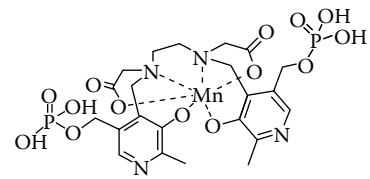

Mn-DPDP (Teslascan®)
Mangafodipir

FIGURE 2.1 Some approved (U.S. or Europe) MRI contrast agents with trade name, generic name, and chemical abbreviation.

Relaxivity is a useful parameter that allows an *in vitro* ranking of various contrast agents. Increased relaxivity typically equates to greater contrast at an equivalent dose, or equivalent contrast at a lower dose. However, *in vivo*, signal change is more complex than the simple linear relationship implied by Equations 2.3 and 2.4. There are both physical and chemical reasons for this that will be described below. First, the chemistry of these contrast agents will be discussed.

2.4 CHEMISTRY OF T_1 AGENTS

MRI contrast agents must be biocompatible pharmaceuticals in addition to nuclear relaxation probes. Because of the relatively high doses used, they should have good water solubility. They should be nontoxic at the dose required to give the required imaging effect; $1/T_1$ changes as small as 10 to 20% can be detected by MRI.

T_1 agents are typically gadolinium(III) complexes, manganese(II) complexes, or, in several animal studies, just the Mn^{2+} cation[3,4] (given as $MnCl_2$; see also Chapter 20 for another Mn^{2+} application). Figure 2.1 shows some contrast agents approved for use in the U.S. and Europe.

Chemically, the gadolinium (Gd) compounds exhibit similar features: an eight-coordinate ligand binding to Gd and a single water molecule coordinated to Gd. The multidentate ligand is required for safety.[5] The ligand encapsulates the gadolinium, resulting in a high thermodynamic stability and kinetic inertness with respect to metal loss. This enables the contrast agent to be excreted intact — an important property since these contrast agents tend to be much less toxic than their individual components. For example, the DTPA ligand and gadolinium chloride both have an LD_{50} of 0.5 mmol/kg in rats (LD_{50} = dose that causes death in 50% of the animals), while the Gd-DTPA complex has nearly a factor of 20 higher safety margin, with an LD_{50} of 8 mmol/kg for the Gd-DTPA complex.[6]

Metal complex stability can be assessed by determining the metal-ligand stability constant (also called the formation constant).[7] Stability constants are typically very high for Gd complexes used as contrast agents,[5] $K > 10^{17}$ M^{-1}. Stability constant determination requires knowledge of the protonation constants, pKa values, of the ligand. A less rigorous but still practical approach is to determine the relative stability compared to that of a known agent. For example, is the complex more or less stable than DTPA or EDTA?

Kinetics is also important. How fast will the complex release the gadolinium? Metal ion release is catalyzed by acid, competing metal ions such as zinc, or other coordinating anions like phosphate. Dissociation rates can be measured absolutely using, for instance, radiochemical[8] or optical methods[9] for detection. Alternately, some relative rate can be measured and compared to a benchmark compound like Gd-DTPA or Gd-DOTA. Vander Elst and colleagues have monitored the change in P-31 relaxation rate as a function of time when a Gd complex is subjected to a cocktail of phosphate groups,[10,11] and ranked the relative inertness of various contrast agents. As a general rule, macrocyclic ligands like DOTA tend to give more kinetically inert complexes than acyclic ligands like DTPA.

To illustrate the importance of both thermodynamic stability and kinetic inertness, consider Gd-DTPA, Gd-DTPA-BMA, and Gd-EDTA. The stability constants[5] for Gd-EDTA and Gd-DTPA-BMA are similar ($K = 10^{17}$) and much lower than for Gd-DTPA ($K = 10^{22.5}$). However, Gd-EDTA has a greater than 10-fold lower LD_{50} than the other two compounds.[12] Biodistribution studies[13] showed that there was more than 25 times as much Gd deposited in the femur (indicative of Gd loss from the complex) of a rat 14 days after Gd-EDTA was injected than when Gd-DTPA-BMA was administered. What may rationalize these findings is that the rate of transmetallation with other metal ions for Gd-DTPA-BMA is about the same as that for Gd-DTPA.[9] Gd-EDTA, on the other hand, is much more labile.[13] This indicates that complexes of lower stability can be used *in vivo* provided that they are kinetically inert.

There is a great deal of literature on the kinetics and thermodynamics of metal complex stability for gadolinium complexes. An excellent review is given by Brücher and Sherry[14] in a book on the chemistry of MR contrast agents. Lanthanide coordination chemistry tends to be very similar, so observations about stability and inertness for other lanthanides, like samarium-153, lutetium-177, and yttrium-90, used in nuclear medicine will also apply to gadolinium.

2.5 PARAMAGNETIC ENHANCED NUCLEAR RELAXATION

The paramagnetic ion and coordinated water molecule are essential to providing contrast. The gadolinium(III) ion has a high magnetic moment and a relatively slow electronic relaxation rate, properties that make it an excellent relaxer of water protons. The proximity of the coordinated water molecule leads to efficient relaxation. The coordinated water molecule is in rapid chemical exchange (10^6 exchanges per second) with solvating water molecules.[15] This rapid exchange leads to a catalytic effect whereby the Gd complex effectively shortens the relaxation times of the bulk solution.

The approved manganese agent, Mn-DPDP (Teslascan, Mangafodipir) does not have a site for coordinating water.[16] However, this compound dissociates *in vivo* and the manganese is taken up

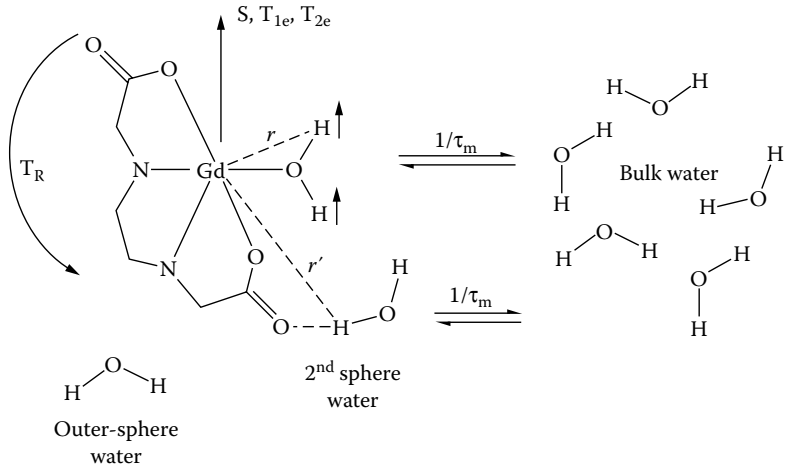

FIGURE 2.2 Molecular parameters that influence inner- and second-sphere relaxivity.

by hepatocytes. In the liver and gall bladder, the Mn(II) ion is bound to macromolecules, resulting in increased relaxivity.[17]

There are two pathways by which the paramagnetic complex enhances water relaxation. There is an inner-sphere effect whereby the metal-bound water is relaxed efficiently and this water undergoes rapid chemical exchange with other solvent water. This relaxation and fast water exchange catalytically enhances the relaxation rate of the bulk water. In addition, water not contained in the first coordination sphere can also be relaxed by the ion. This water is classified into two groups: second-sphere water, which denotes water molecules that directly hydrate the complex and have a lifetime in the second sphere longer than the time constant for water diffusion, and outer-sphere water, which is not associated with the complex but is diffusing nearby. Second- and outer-sphere water for this discussion are termed outer sphere. The different classes of water and the molecular parameters that determine relaxivity are shown in Figure 2.2. Relaxivity can be separated into inner- and outer-sphere relaxivity, r_1^{IS} and r_1^{OS}, respectively, and this is useful for understanding the biophysics behind the relaxation enhancement.

$$r_1 = r_1^{IS} + r_1^{OS} = \frac{q/[H_2O]}{T_{1m} + \tau_m} + r_1^{OS} \tag{2.5}$$

Here q is the number of water molecules in the inner sphere, T_{1m} is the relaxation time of these inner-sphere water protons, and τ_m is the lifetime of these waters in the inner sphere (the reciprocal of τ_m is the water exchange rate, $k_{ex} = 1/\tau_m$). Relaxivity depends directly on how many water molecules are coordinated, and inversely on the relaxation time of the bound water and how long it is bound. The relaxation rate at typical imaging fields for water protons bound to Gd or Mn is given by Equation 2.6:

$$\frac{1}{T_{1m}} = \frac{2}{15}\frac{\gamma_H^2 g_e^2 \mu_B^2 S(S+1)}{r_{M-H}^6}\left[\frac{3\tau_c}{1+\omega_H^2\tau_c^2}\right] \tag{2.6}$$

$$\frac{1}{\tau_c} = \frac{1}{\tau_R} + \frac{1}{T_{1e}} + \frac{1}{\tau_m} \tag{2.7}$$

Paramagnetic relaxation ($1/T_{1m}$) occurs via a dipolar mechanism. Relaxation depends on the spin quantum number (S), some fundamental constants (magnetogyric ratio, Bohr magneton, electronic g factor, $g_e = 2$ for Gd(III) and Mn(II)), the metal-to-hydrogen (M-H) distance, r_{M-H}, the proton Larmor frequency ω_H (in rad/sec), and a correlation time τ_c. The product $S(S + 1)$ is proportional to the magnetic moment. All other factors being equal, the higher the magnetic moment, the more efficient the relaxation. This is why Gd^{3+} ($S = 7/2$) is preferred to an ion such as copper (Cu^{2+}, $S = 1/2$). The dipolar effect depends on the distance between the ion and the hydrogen nucleus, r_{MH}, to the inverse sixth power. The inner-sphere water is critical; it has the shortest metal-to-hydrogen distance of water hydrating the metal complex. Mn^{2+} has a lower spin number ($S = 5/2$) than Gd^{3+}, but Mn^{2+} is a small ion and has a shorter Mn-H distance. Curiously, the $S(S + 1)/r^6$ term is approximately equal for Mn^{2+} and Gd^{3+}.

Fluctuating magnetic dipoles can induce spin transitions and cause spin relaxation. A correlation time is a time constant for characterizing these fluctuations; its reciprocal, $1/\tau_c$, is the average rate constant for these fluctuating dipoles. The closer this rate is to the Larmor frequency, the more efficient the relaxation. There are several processes that lead to fluctuating magnetic dipoles. Electronic relaxation ($1/T_{1e}$) at the Gd(III) ion creates a fluctuating field. Rotational diffusion ($1/\tau_R$) of the complex creates a fluctuating field. Water exchange ($1/\tau_m$) in and out of the coordination sphere creates a fluctuating field for the hydrogen nucleus. It is the fastest rate (shortest time constant) that determines the extent of relaxation (Equation 2.7). For most Gd(III) and Mn(II) complexes at imaging field strengths, it is rotational diffusion that is the dominant correlation time. The terms in square brackets are sometimes referred to as dispersive because once $\omega^2\tau_c^2 > 1$, the relaxation rate becomes slower and disperses with increasing frequency (field).

Mn(II) and Gd(III) are chosen as relaxation agents because electronic relaxation ($1/T_{1e}$) is slow, the magnetic moment is large, and water exchange is typically fast. To illustrate the effect of rotational diffusion and the field dependence on relaxivity, consider two similar compounds shown in Figure 2.1: Gd-DTPA and MS-325. MS-325 has the same Gd-binding ligand but also has a lipophilic group that enables it to bind to serum albumin. Small molecules like Gd-DTPA tumble very fast, in the gigahertz range (1 GHz = 1000 MHz), but the Larmor frequency for protons at imaging fields is much slower. For example, at 1.5 tesla, the Larmor frequency is about 65 MHz, so relaxation is not as efficient as it could be. Larger molecules like proteins tumble much more slowly. When contrast agents are made to tumble more slowly, relaxivity is increased. Lauffer[18] pointed out that if small contrast agents could be made to bind noncovalently to protein targets, then their relaxivity would be increased upon binding because the contrast agent would take on the rotational characteristics of the protein. This was termed receptor-induced magnetization enhancement (RIME). MS-325 is an example of a contrast agent designed to exploit the RIME effect.[19] In the absence of albumin, the relaxivity of MS-325 is about 50% greater than Gd-DTPA because its larger size results in a slower tumbling rate, but in the presence of albumin, the relaxivity is about 600% greater than Gd-DTPA at 1.5 tesla. This is illustrated in Figure 2.3, where the magnetic field dependence on relaxivity is plotted for MS-325 (circles) and Gd-DTPA (squares) in either serum albumin solution (filled symbols) or buffered saline (open symbols).

Figure 2.3 also shows that the relaxivity is rather field independent for Gd-DTPA and MS-325 in buffer, but the relaxivity of MS-325 bound to protein first increases and then decreases with field. At high fields, the inequality $\omega_H^2\tau_c^2 > 1$ is reached and T_{1m} will become longer (and relaxivity lower) with increasing field. The relaxivity first increases because the correlation time can also change with field. At low fields, electronic relaxation is very fast and the correlation time, τ_c, is approximately T_{1e}. The electronic relaxation rate for Gd(III) and Mn(II) decreases with the square of the magnetic field, so as field is increased, τ_c is getting longer and relaxivity increases. At some point, the rate of rotational diffusion is the fastest process and τ_c becomes τ_R. The field at which T_{1e} no longer dominates the correlation time will depend on the complex and the rotational correlation time. However, it appears safe to say that at 1.5 tesla and above, rotational motion is the correlation time that defines relaxivity.

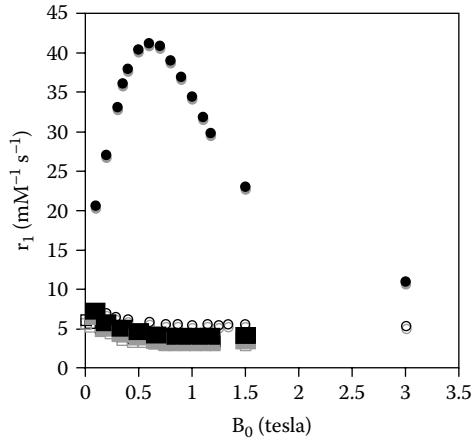

FIGURE 2.3 Magnetic field dependence on relaxivity for MS-325 (circles) and Gd-DTPA (squares) in either serum albumin solution (filled symbols) or buffered saline (open symbols) at 37°C.

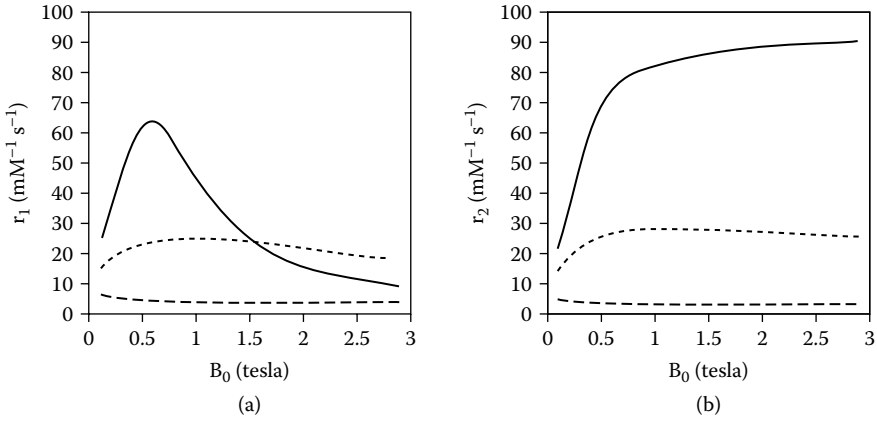

FIGURE 2.4 Effect of rotational correlation time on longitudinal (r_1) (a) and transverse (r_2) (b) relaxivities as a function of field strength. Long correlation time (τ_R = 10 nsec, —) typical of albumin binding gives high r_1 that decreases with increasing field and high r_2; intermediate correlation time (τ_R = 1 nsec, ---) shows relaxivity maximum for r_1 pushed out to higher field; short correlation time (τ_R = 0.1 nsec, ---) typical of ECF agents shows low, roughly field independent r_1, r_2. Simulations with other parameters typical of Gd-based agents.[22]

Transverse relaxivity can also be factored into inner- and outer-sphere terms. For Gd(III) and Mn(II), T_{2m} is predominantly governed by a dipolar mechanism (at very high fields, another mechanism called Curie spin relaxation[20,21] also shortens T_2). T_{2m} is given by Equation 2.8, which is very similar to that of Equation 8.6 for longitudinal relaxation, except that there is also a nondispersive term inside the square brackets.

$$\frac{1}{T_{2m}} = \frac{1}{15}\frac{\gamma_H^2 g_e^2 \mu_B^2 S(S+1)}{r_{M-H}^6}\left[4\tau_c + \frac{3\tau_c}{1+\omega_H^2\tau_c^2}\right] \tag{2.8}$$

Figure 2.4 further illustrates the effect of correlation time and field strength on relaxivity. In Figure 2.4, r_1 and r_2 are simulated over a range of fields encountered in MRI for correlation times of 0.1 nsec (typical of extracellular fluid, ECF, agents), 1 nsec (intermediate motion), and 10 nsec

TABLE 2.1
Relaxivities[68] (mM^{-1}sec^{-1}) of Selected Contrast Media (0.25 mM) in Plasma at 0.47, 1.5, and 3 Tesla at 37°

Compound		0.47 Tesla		1.5 Tesla		3 Tesla	
Chemical/Code	Commercial	r_1	r_2	r_1	r_2	r_1	r_2
Gd-DTPA	Magnevist	3.8	4.1	4.1	4.6	3.7	5.2
Gd-DTPA-BMA	Omniscan	4.4	4.6	4.3	5.2	4.0	5.6
Gd-HPDO3A	Prohance	4.8	6.1	4.1	5.0	3.7	5.7
Gd-DOTA	Dotarem	4.3	5.5	3.6	4.3	3.5	4.9
Gd-EOB-DTPA	Primovist	8.7	13	6.9	8.7	6.2	11.0
Gd-BOPTA	MultiHance	9.2	12.9	6.3	8.7	5.2	11.0
MS-325[a]	Vasovist	47.2	57.6	27.7	72.6	9.9	73
Gadomer		19	23	16.0	19.0	13.0	25
AMI-25	Endorem Feridex	NA	NA	4.5	33	2.7	45
SHU-555A	Resovist	15	101	7.4	95	3.3	160
SHU-555C	Supravist	22.3	99	10.7	38	5.6	95

Note: NA = not available.
[a] Data from Eldredge et al.[23]

(typical of albumin-bound agents). Figure 2.4 shows that the benefits of very slow rotation are seen at lower field strengths. Note also that r_1 does not go to zero because there is an outer-sphere component to relaxivity[22] and the correlation times that govern outer-sphere relaxivity are quite short. r_2 is always greater than r_1, and for very slow tumbling systems, the r_2/r_1 ratio becomes large at high fields. Electronic and nuclear relaxation are described in greater detail in various reviews and books.[5,20]

Figure 2.4 suggests that slow tumbling T_1 agents become less effective at high fields, but one must also recall that relaxation times for tissue are longer at high fields and that signal-to-noise ratio (SNR) increases with increased field. These factors and the choice of sequence mean that a contrast agent with a lower relaxivity at 3 T than 1.5 T may still provide greater contrast at 3 T than at 1.5 T. Table 2.1 lists relaxivities for some widely studied gadolinium complexes in plasma at 0.5, 1.5, and 3 tesla. The ECF agents show little field dependence, while the slow tumbling compounds Gadomer and MS-325 (albumin bound in plasma) and the iron oxide particles show strong field dependence.

The MS-325 example clearly shows the importance of chemical speciation on observed relaxation rates. Obviously, if the fraction of the contrast agent bound to the macromolecule is lower, then the observed relaxivity will also be lower. Contrast agents such as Gd-BOPTA (MultiHance, gadobenate) are only about 10% bound to plasma proteins and have relaxivities intermediate between albumin-bound MS-325 and ECF agents (Table 2.1). For compounds with reversible protein binding, the relaxivity observed will no longer be independent of concentration,[23] because changes in concentration will shift the equilibrium between free and bound. As a result, the fraction of MS-325 bound to albumin immediately after a bolus injection will be lower than that after the compound has distributed because the high concentration present in the bolus will saturate the albumin.[24]

Other chemical effects can also alter relaxivity *in vivo*. For instance, increasing q promises to increase relaxivity, and this is generally true in pure water.[25,26] However, increasing the number of waters bound also opens up a cleft around the metal ion that can allow other ligands to bind. Endogenous citrate, phosphate, and bicarbonate have high affinity for gadolinium.[27] When these ligands bind, they displace the bound water molecules and actually decrease relaxivity. This effect is typically only seen in $q \geq 2$ complexes, presumably because when there is only one water bound, there is not enough space near the metal ion to accommodate the larger bicarbonate or phosphate ion.

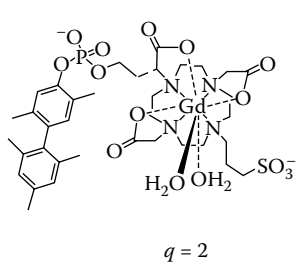

(a) PBS, pH 7.4, 37°C. r_1 = 9.1 mM^{-1} s^{-1} at 20 MHz

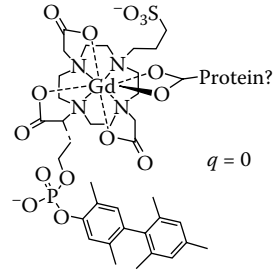

(b) PBS, pH 7.4, 37°C, 0.66 mM HSA, 0.1 mM Gd. Compound > 99% bound to HSA, r_1 = 12.3 mM^{-1} s^{-1} at 20 MHz

FIGURE 2.5 Gadolinium complex where $q = 2$ in buffered solution but $q = 0$ when bound to a protein. Hydration state suggested by relaxivity and confirmed by ^{1}H ENDOR.

Protein binding can also have an effect on q. For instance, Zech et al.[25] showed that the albumin binding $q = 2$ derivative shown in Figure 2.5 had high relaxivity in phosphate-buffered saline (PBS), but the expected relaxivity boost was missing in the presence of human serum albumin (HSA), even though the complex had high affinity to albumin. Electron-nuclear double resonance (ENDOR) spectroscopy showed that the two water molecules were displaced when the complex was bound to serum albumin, accounting for the lower than expected relaxivity. Presumably a protein side chain (Asp, Glu?) with high local concentration coordinated the Gd ion and displaced the waters. When europium is used as a surrogate for gadolinium, fluorescence lifetime measurements can also reveal hydration number changes.[27,28]

Chemical exchange of water in and out of the first coordination sphere is another parameter that can have a significant effect on relaxivity. The water residency time, τ_m, appears in the denominator of Equation 2.5 as $(T_{1m} + \tau_m)$. For fast tumbling molecules like Gd-DTPA, relaxation is less efficient because of rotational motion and $T_{1m} > \tau_m$. As a result, the first generation of clinical contrast agents all have similar relaxivities because their size is about the same, meaning T_{1m} is similar. However, the compounds in Figure 2.1 all have different water exchange rates. When T_{1m} is reduced, τ_m can become important and may limit relaxivity. For instance, when DTPA is converted into the bis(amide) DTPA-BMA, the water exchange rate at gadolinium is reduced by a factor of 10. For Gd-DTPA and Gd-DTPA-BMA, fast rotation means that T_{1m} is on the order of 10 μsec at 1.5 tesla. If T_{1m} is reduced by slowing down tumbling, say by protein binding, then T_{1m} is reduced to 0.7 μsec. In this scenario, the slow water exchange at the Gd-DTPA-BMA chelate would significantly limit its relaxivity.

Interaction with a protein target can also affect water exchange. Eldredge et al.[23] found that the relaxivity of MS-325 was different when bound to serum albumins of different species. For instance, relaxivity was almost twice as high when MS-325 was bound to human serum albumin than when bound to rabbit serum albumin. Based on variable temperature and variable field relaxivity measurements, they postulated that water exchange at MS-325 was slower when MS-325 was bound to rabbit serum albumin than when MS-325 was bound to human serum albumin.

The molecular factors that serve to increase or decrease r_1 will affect r_2 in the same way. However, T_2-weighted agents are typically used because of their susceptibility (T_2*) effect, rather than the pure T_2 shortening, as will be discussed below. It should be clear that relaxivity is not a constant, but depends strongly on environment. It is important to measure r_1 and r_2 under the conditions where the contrast agent will be used (magnetic field, physiological temperature, tissue) in order to better understand its effect *in vivo*.

When manganese is given as the simple salt $MnCl_2$, its relaxivity in water will be quite different than in the *in vivo* situation. Manganese is known to accumulate in the liver, where it has a high

TABLE 2.2
Relaxivities ($mM^{-1}sec^{-1}$) of Mn^{2+} in the Presence of Various Proteins[29] and Chelators[30] (Figure 2.6) at 0.47 Tesla and 25°C

Chelator Type	Protein	r_1	Hydration Number, q
None	None	9.0	6
None	Pyruvate kinase	275	?
None	Concanavalin A	96	?
None	Carboxypeptidase	43	?
EDTA derivative	None	6.4	1
DTPA derivative	None	3.5	0
EDTA derivative	Human serum albumin	55.9	1
DTPA derivative	Human serum albumin	4.9	0

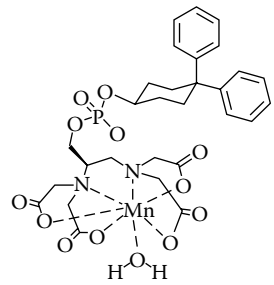

Mn-EDTA derivative
$q = 1$

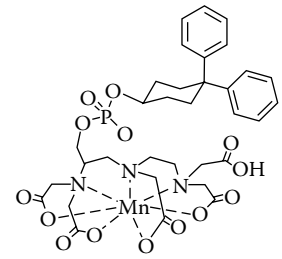

Mn-DTPA derivative
$q = 0$

FIGURE 2.6 Serum albumin-binding derivatives of manganese(II). The EDTA derivative (left) has one inner-sphere water while the DTPA derivative has no site available for direct water coordination, $q = 0$

relaxivity due to binding to macromolecules. The mechanism of action of Mn-DPDP is dissociation of the complex releasing free Mn^{2+} into the hepatocytes, resulting in manganese bound to macromolecules and increased relaxivity.[17] In his excellent review on contrast agents,[29] Lauffer listed relaxivities of Mn(II) bound to several proteins, and relaxivity can vary over two orders of magnitude. The speciation of manganese is critical to understanding its contrast-enhancing behavior. Table 2.2 illustrates this point. The relaxivity of the aqua ion is increased in the presence of proteins, but the choice of protein is also critical. Troughton et al.[30] recently described Mn(II) complexes of EDTA or DTPA ligands that were derivatized with the same albumin-binding group used with MS-325 (Figure 2.6). The Mn-EDTA derivative has one inner-sphere water, while the Mn-DTPA derivative does not have a water bound. As expected, protein binding has a large impact on the Mn-EDTA derivative but not on the $q = 0$ Mn-DTPA compound; these relaxivities are also listed in Table 2.2.

2.6 T_2 AGENTS

Paramagnetism generally involves the magnetism of small isolated ions that only behave as local magnets in the presence of an external magnetic field. For paramagnetic materials that contain multiple ions, the total magnetic susceptibility is directly proportional to the number of ions in

the material. Therefore, the molar magnetic susceptibility (magnetic susceptibility divided by the number of ions) is constant. There are other materials that exhibit ferromagnetism and superparamagnetism. For certain materials such as ferrite (iron oxide) the individual spins of each iron cooperatively, via quantum mechanical interactions, build up to give the crystal a very large total spin, resulting in a very large molecular magnetic susceptibility that is a function of the number of spins. Such a material is called ferromagnetic, and its magnetism persists outside the external magnetic field. A weaker form of this is superparamagnetism: small particles of iron oxide with aligned spins in a magnetic field. Since the particles are small (submicron), the magnetic susceptibility effect is smaller than for large crystals of ferrites. Superparamagnets are no longer magnetic outside of the external field. These iron oxide particles represent an important class of contrast agents.[31]

The iron oxide particles consist of a core of one or more magnetic crystals of Fe_3O_4 embedded in a coating. Because these are materials, there is a distribution of sizes. Ultrasmall particles of iron oxide (USPIOs) have a single crystal core and a submicron diameter (e.g., ferumoxtran (Sinerem, Combidex, or AMI-227) has a crystal diameter of 4.3 to 4.9 nm and a global particle diameter of ca. 50 nm).[32] Small particles of iron oxide (SPIOs) have cores containing more than one crystal of Fe_3O_4 and are larger than USPIOs but still submicron (e.g., ferumoxide (Endorem, Feridex, or AMI-25) has a crystal diameter of 4.3 to 4.8 nm and a global particle diameter of ca. 200 nm).[32] USPIOs and SPIOs are small enough to form a stable suspension and can be administered intravenously. The size differences result in differences in pharmacokinetic behavior, which will be described below. There are also large particles that are used for oral applications (e.g., Abdoscan, 50-nm crystals making up a 3-μm particle).[33] USPIOs are also referred to as microcrystalline iron oxide nanoparticles (MIONs).

There are no inner-sphere water molecules in iron particles, and relaxation of water arises from the water molecules diffusing near the particle. However, the mechanism of outer-sphere relaxation is different than described above. One feature is that the crystals have a net magnetization, and as the external field is increased, this magnetization is increased (this is true as well for Gd, but the effect is much smaller). The modulation of this net magnetization can cause proton relaxation (so-called Curie spin relaxation). The theories describing the field dependence of iron oxide relaxivity have been reported.[33] Solvent relaxation induced by iron oxide systems is complex. Bulte et al.[34,35] used a combination of variable field T_2 measurements (T_2 relaxometry), electron paramagnetic resonance (EPR), and magnetization measurements to fully characterize one such USPIO, MION-46L. To fully explain their experimental findings, they proposed the existence of three different magnetic phases for this USPIO: a superparamagnetic core, an antiferromagnetic ferritin-like phase of incompletely converted iron oxyhydroxide, and a paramagnetic surface effect of ferric ions.

There are some generalities about relaxivity in these particles. For the USPIOs, longitudinal relaxivity (r_1) can be quite high and these can function as effective T_1 agents. The r_2/r_1 ratio for USPIOs is significantly larger than for gadolinium complexes, and r_2/r_1 increases with increasing magnetic field. When there is aggregation of crystals, which is the case in SPIOs, longitudinal relaxivity tends to decrease (r_1 drops) and transverse relaxivity increases (r_2 increases). Thus, for both the particles themselves and aggregates of particles the ratio of r_2/r_1 typically increases as the size of the particles or aggregates increases, though the T_2 relaxivity as a function of particle size can be quite complicated. See, for example, Weisskoff et al.[36] and Hardy and Henkelman.[37] The effect of aggregation of crystals is that the aggregate itself can be considered a large magnetized sphere whose magnetic moment increases with increasing field strength. This gives rise to susceptibility effects and the SPIOs can act as T_2* relaxation agents. This has important consequences when considering the effects of contrast agent compartmentalization on imaging (see below).

There is also a speciation effect on relaxivity for iron particles. When these nanoparticles cluster together, transverse relaxivity, r_2, increases. This phenomenon has been exploited by Perez et al., who have created sensors based on assembling and disassembling these nanoparticle clusters.[38,39]

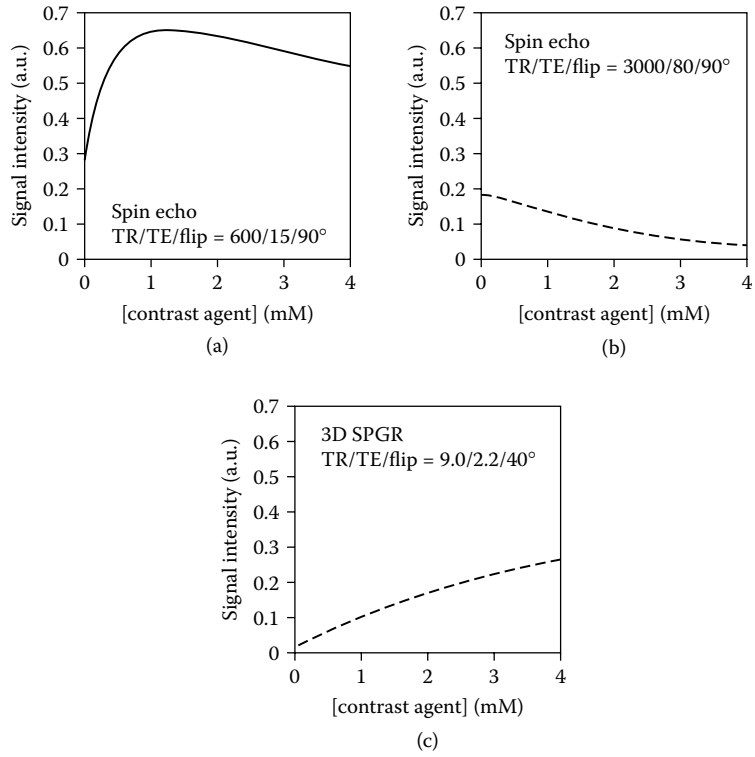

FIGURE 2.7 Effect of contrast agent on image intensity (baseline T_1, T_2 typical of muscle) on T_1- and T_2-weighted scans. (a) T_1-weighted spin echo (TR = 600 msec) shows linear increase of signal only for contrast agent concentration less than 0.5 m*M*. (b) T_2-weighted spin echo images (TR = 3000 msec) shows only T_2 signal loss effects due to contrast agent with no T_1 enhancement because of long TR. (c) Typical short-TR fast spoiled gradient echo sequence. The very short TE and short TR give monotonically increased image intensity across the entire range of contrast agent concentrations typically found in clinical scans.

2.7 IMAGING PHYSICS: T_1 AND T_2 AGENTS

Contrast agent behavior *in vivo* is quite complex. Even in the simple case of a single compartment with pure linear relaxation, the effect of the contrast agent on the MR image is generally nonlinear. In traditional spin echo sequences nonlinearity can be a result of T_1 saturation or T_2 signal loss. Once the contrast agent shortens $T_1 < TR/2$, increasing the contrast agent concentration will have little effect on increasing the available longitudinal magnetization because the tissue will have nearly fully recovered the magnetization before the next rf pulse. Because contrast agents affect both T_1 and T_2 relaxation, at high enough concentration the contrast agent will reduce T_2 to the order of TE, and will then decrease MR image intensity. These effects are illustrated in Figure 2.7, where signal intensity is plotted vs. contrast agent concentration for T_1- and T_2-weighted spin echo sequences. Figure 2.7 was generated assuming a contrast agent relaxivity of 4 $mM^{-1}sec^{-1}$, typical of most commercial ECF gadolinium agents, and tissue relaxation times typical of muscle (T_1 = 1200 msec, T_2 = 50 msec). For the T_1-weighted sequence (TR/TE = 600/15) (Figure 2.7a), signal intensity begins to level out at a contrast agent concentration between 0.5 and 1.0 m*M*; this is the range where the T_1 has dropped to around 300 msec, or TR/2. At concentrations above 1 m*M*, the T_1 effect is saturated, and the only *imaging* effect of the contrast agent is to make T_2 shorter and cause signal loss, even on this T_1-weighted sequence. Signal is lost because even a T_1-weighted sequence has a finite TE, and T_2 effects enter when T_2 is short enough.

The signal intensity plateau on the T_2-weighted scan (TR/TE = 3000/80) (Figure 2.7b) occurs at much lower contrast agent concentration. Because TR is so long, the only real effect of the contrast agent is to reduce (rather than increase) signal intensity on this T_2-weighted scan. T_2 agents create negative contrast exactly by providing enhanced T_2 relaxation, and thus darker images on T_2-weighted scans.

Increasing the relaxivity (r_1 or r_2) will have the effect of pushing the simulated curves in Figure 2.7a to the left, that is, peak signal and subsequent signal loss will occur at lower contrast agent concentrations. A more linear response of signal to contrast agent can be achieved with a fast three-dimensional spoiled gradient echo (3D SPGR) sequence. This is illustrated in Figure 2.7c, where signal intensity is plotted vs. contrast agent concentration using the same tissue relaxation times and relaxivities as in Figure 2.7a and b for a typical fast 3D SPGR sequence, TR/TE/flip = 9.0/2.2/40°. The short TR and very short TE ensure that signal intensity increases across the entire concentration range. At high concentration the effect of the contrast agent is becoming nonlinear, but the signal is still increasing with increasing contrast agent concentration.

However, in tissue, relaxation itself is usually nonlinear. The extent to which a metal complex influences tissue relaxation rates depends on three factors:

1. The chemical environment encountered by the metal complex. Binding of the agent to macromolecules can cause significant relaxivity enhancement. Similarly, clustering of nanoparticles can strongly alter r_2. This was discussed in detail above for both T_1 and T_2 agents.
2. Compartmentalization of the metal complex in tissue. Generally, tissue water is compartmentalized into intravascular, interstitial (fluid space between cells and capillaries), and intracellular space constituting roughly 5, 15, and 80% of total water, respectively. Cellular organelles further subdivide the intracellular component. If water exchange between any of these compartments is slow relative to the relaxation rate in the compartment with the longest T_1, multiexponential relaxation may result. This can decrease the effective tissue relaxivity of an agent because not all of the tissue water is encountering the paramagnetic center.
3. The magnetic susceptibility of the contrast agent. The contrast agent causes a microscopic field inhomogeneity on a biological scale of 10 to 1000 nm rather than on the chemical scale of 0.1 to 1 nm. This results in a reduction in apparent T_2.

Chemical speciation was discussed above. For molecular and cellular imaging it is useful to consider physical compartmentalization and magnetic susceptibility in more detail. Physical compartmentalization makes it more difficult to predict tissue relaxivity. With the exception of opsonization of iron oxide particles,[40] the liver-specific agents,[41] and specific cell-labeling preparations (see, e.g., Chapter 18), most contrast agents are designed to stay out of cells. Often the contrast agent will be localized to extracellular spaces. As a result, the simple relaxivity equations do not necessarily hold. For a Gd-based ECF agent in a test tube, it takes about 3 μsec for water to diffuse between Gd molecules;[42] in the time of a typical imaging TR, a given water molecule may interact with thousands or millions of Gd molecules, and all water molecules will interact with approximately the same number of Gd ions. However, if that same ECF agent is compartmentalized solely within the microvasculature, it takes between 2 and 20 sec for most of the water in the tissue (85% of it is extravascular) to physically diffuse into the microvasculature; most of the water in the tissue does not have the opportunity to be relaxed by the Gd within the TR of an imaging acquisition, resulting in a lower signal enhancement than that predicted by Equation 2.3 and assuming a uniform distribution of contrast agent throughout the tissue.

To deal with compartmentalization, the concept of water exchange and exchange time, τ, between compartments is often used.[43,44] The water exchange rate and the size of the compartments will determine the effect of the contrast agent on MRI signal. To illustrate this phenomenon, the two

limiting cases of exchange will be described. For more detail, the reader should consult reviews on this topic.[42,44] In one extreme, water moves so fast between the biological compartments that the net effect is as if the contrast agent were uniformly spread throughout the whole tissue. This regime, called fast exchange, occurs whenever the exchange rate, $1/\tau$, between the compartments is much faster than the difference in relaxation rates between the compartments.[45] This occurs in blood where the red cell has a short water exchange time, on the order of 5 to 10 msec.[46] The intact red cell prevents most MR contrast agents from entering the cell, but as long as the plasma T_1 is longer than 20 msec, the two compartments of the blood (plasma + red cells) are in fast exchange and blood behaves for MR purposes as if the contrast agent were spread uniformly through the blood. In this case, the effective relaxation rate will be the weighted average of the relaxation in the two compartments. That is, if for compartment i (where $i = a, b$) the volume fraction is f_i, the initial T_1 is T_{1i}, and the concentration of agent is C_i (which could be zero), the whole tissue together will behave like

$$\frac{1}{T_1} = f_a\left(\frac{1}{T_{1a}} + r_{1a}C_a\right) + f_b\left(\frac{1}{T_{1b}} + r_{1b}C_b\right) \tag{2.9}$$

In slow exchange, the water exchange rate is much slower than the difference in relaxation rates between the compartments. In this case, a single relaxation time, and thus a single relaxivity, is meaningless, because the two microscopic compartments will relax with their own relaxation times. Very few biological compartments show true slow exchange, except at extremely high concentrations of contrast agent. The intermediate case, when exchange is neither slow nor fast (intermediate exchange), occurs very commonly. With intermediate exchange, relaxation behavior appears biexponential, although both the apparent compartment size and the effective T_1 of the two compartments will vary from their true biological size and T_1. It is possible to model the signal intensity behavior as a function of contrast agent concentration to estimate water exchange times *in vivo*. Although characterizing human tissue as having only one or two compartments is an oversimplification, these types of models have proved useful for explaining the effects of biological water mobility on contrast-enhanced scans.[47]

Biological compartmentalization also results in susceptibility contrast. The contrast agent causes microscopic field inhomogeneities sometimes called mesoscopic inhomogeneities.[48] Water diffusion causes the protons to dephase from one another due to the different magnetic fields that they experience during their random walks. Even in the absence of water diffusion, the field inhomogeneity causes intravoxel dephasing, and thus signal loss on gradient echo images due to the different microscopic magnetic fields within the voxel. The strength of the perturbing magnetic field is directly proportional to contrast agent concentration and its molar magnetic susceptibility (χ). The actual magnitude and even direction of the magnetic field shifts depend strongly on the size and shape of the biological compartment in which the contrast agent resides;[48] the size of the susceptibility contrast effect depends on how the water diffuses through the tissue.

The susceptibility T_2 effect is not limited by compartmentalization. For example, first-pass brain perfusion imaging[49] relies on the susceptibility effect of currently approved extracellular Gd-based agents. The blood volume in the brain is very small (4% in gray matter, 2% in white matter), and slow water exchange between the extravascular and intravascular spaces in the brain limits the size of signal changes due to any T_1-based contrast agent at acceptable doses. The susceptibility-based T_2 and T_2* effects can be much larger — as much as a 50% signal drop in normal gray matter at the same dose — due to the "action at a distance" effect possible with the outer-sphere effect. Thus, in cases of slow exchange and when only small compartments are available for the contrast agent, susceptibility contrast may be the medically relevant contrast mechanism of choice. Iron oxide particles with their much higher magnetic susceptibility are more potent susceptibility agents.

Physical compartmentalization and magnetic susceptibility influence how relaxation manifests itself in labeled cells. For T_1 agents, compartmentalization plays an important role. Terreno et al.[50]

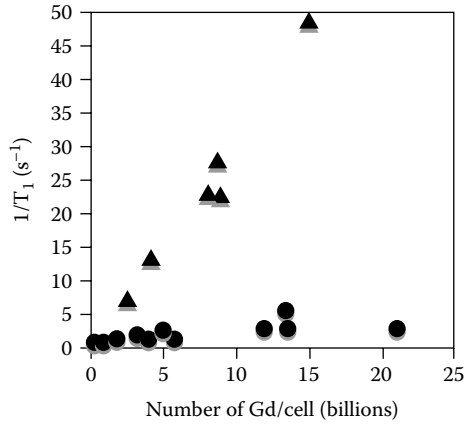

FIGURE 2.8 Effect of compartmentalization on observed T_1. Gd-HPDO3A introduced into cells via electroporation is distributed throughout the cytosol, resulting in efficient relaxation of intracellular water (triangles). Gd-HPDO3A introduced via pinocytosis sees the Gd localized in vesicles. Slow water exchange in and out of the vesicle limits the T_1 lowering effect of the contrast agent (circles).

recently showed that when Gd-HPDO3A was incorporated into rat hepatocarcinoma cells, the method of internalization influenced the observed water relaxation rates. If the gadolinium complex is internalized by pinocytosis, the complex is trapped inside intracellular vesicles. On the other hand, if electroporation is used, then the gadolinium complex is distributed throughout the cytoplasm. When the compound was trapped in vesicles, the observed relaxation rate increased with increasing Gd/cell and then reached a plateau (Figure 2.8 circles). This behavior is typical of intermediate to slow water exchange as the contrast agent concentration increases. Increased gadolinium concentration no longer has any effect on T_1 since water exchange through the vesicle is too slow to affect the other intracellular water. On the other hand, when the compound was distributed throughout the cytoplasm, the relaxation rate increased more quickly (greater slope, Figure 2.8 triangles) with increasing Gd/cell and did not reach a plateau, since the gadolinium was relaxing most of the intracellular water.

When cells are labeled with iron particles, the distribution of the iron particles does not affect the contrast because this is a through-space susceptibility-based relaxation mechanism.

2.8 PARACEST AGENTS

A more recent approach to providing contrast is a magnetization transfer technique termed chemical exchange saturation transfer (CEST) (Chapters 5 and 6). The magnetization transfer (MT) effect that is used clinically exploits a pool of hidden water in some tissues. Water protons associated with macromolecules (e.g., hydrogen bonded to protein and membrane surfaces) have restricted mobility and, because of this, have short T_2. This short T_2 results in a very broad line width of several kilohertz. Mobile water, which makes up most of the tissue, has a relatively long T_2 and a narrow line width. This is illustrated in Figure 2.9a, where magnetization is plotted as a function of frequency. If an rf pulse is applied at a frequency significantly different from the liquid water resonance (e.g., >1 kHz), then the hidden water can become saturated. This hidden water exchanges magnetization with the mobile water via chemical exchange and dipolar coupling. As a result, part of this saturation is transferred to the mobile water peak. This loss of magnetization results in signal loss, as shown in Figure 2.9b. The MT effect can provide contrast since different tissues exhibit MT effects of different magnitudes.

Similarly, magnetization (or saturation) transfer can also be used with contrast agents that have exchangeable hydrogens. Exchangeable hydrogens are typically N-H or O-H hydrogens on molecules

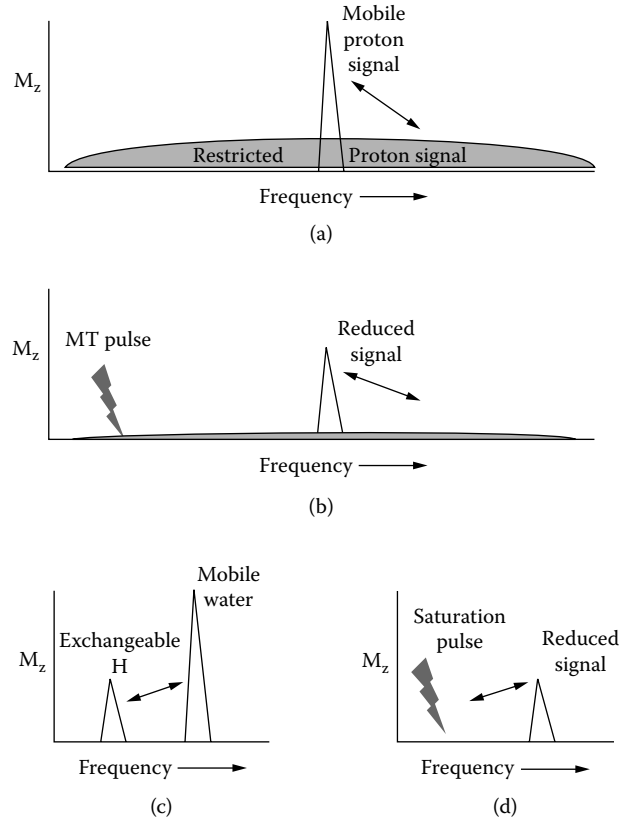

FIGURE 2.9 Magnetization transfer and the CEST effect. (a) Mobile water protons have a relatively long T_2 and resonate over a narrow range of frequencies. There is also a pool of protons with restricted mobility that have a short T_2 and resonate over a wide frequency range. (b) Application of an off-resonance MT pulse saturates the restricted pool, and some of this saturation is transferred to the mobile pool because of chemical exchange and dipolar coupling, resulting in a reduction in magnetization of the mobile pool — this is the MT effect. (c) NMR spectrum of an exchangeable hydrogen with a long T_2 and mobile water. (d) When a saturation pulse is applied at the frequency of the exchangeable hydrogen, this resonance is saturated; chemical exchange results in loss of magnetization of the mobile water — this is the CEST effect.

or exchangeable water molecules from metal complexes. The exchangeable hydrogen has a relatively long T_2 and a narrow line width, but because it is chemically different than water, it resonates at a different frequency (Figure 2.9c). If an rf pulse is applied at the frequency of the exchangeable hydrogen, this resonance becomes saturated (Figure 2.9d). If the hydrogen is undergoing chemical exchange with water, then some of this saturation is transferred to the water, generating negative contrast (Figure 2.9d). This is the CEST effect.[51] CEST differs from the general MT effect because it is only observed when the saturating rf pulse is at the frequency of the exchangeable water. If a different frequency is used, no effect is seen. In the MT effect, the hidden water resonance is so broad that it is excited over a broad range of frequencies. The CEST effect is attractive because it offers the possibility of a contrast agent that can only be observed if the correct pulse sequence is used, in other words a contrast agent that can be turned on and off.

It is intuitive that the rate of chemical exchange should be as fast as possible to maximize the CEST effect. However, the exchangeable hydrogen must resonate at a frequency different from that of water. In order for this to occur, the rate of exchange must be in the slow-exchange regime and the inequality $\Delta\omega\tau > 1$ must be met. Here $\Delta\omega$ is the chemical shift difference in frequency units between the exchangeable hydrogen (labeled ω_A in Figure 2.10) and the pure water resonance, ω_B.

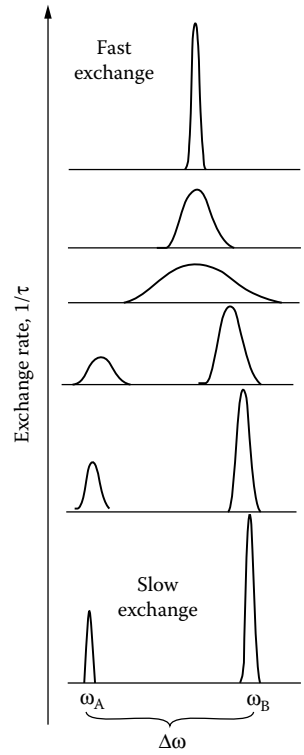

FIGURE 2.10 Effect of chemical exchange rate on the NMR spectrum of an exchangeable hydrogen with chemical shift ω_A and water (ω_B). In slow exchange, $\omega\tau > 1$, two peaks are observed. As $1/\tau$ increases, the peaks coalesce, and at fast exchange, $\omega\tau << 1$, there is a single peak resonating at a frequency that is the population-weighted average between ω_A and ω_B.

τ is the average time that the exchangeable hydrogen spends on its molecule; $1/\tau$ is the rate of hydrogen exchange. If this slow-exchange condition is not met, then only one resonance is observed in the spectrum at a frequency somewhere between the resonance of the water and the exchangeable hydrogen; the exact frequency depends on the relative population of the two groups of hydrogens. The effect of chemical exchange on the resonances is shown in Figure 2.10.

To increase the CEST effect, the number of exchangeable hydrogens can be increased. In this manner, polymeric agents with repeatable units of exchangeable hydrogens have been used.[52,53] The CEST efficiency can be improved by moving to faster exchanging systems that still meet the $\Delta\omega\tau > 1$ requirement. $\Delta\omega$ can be increased by going to higher fields since chemical shift in frequency units (hertz or radians/second) is directly proportional to applied field. Another way to increase $\Delta\omega$ is to incorporate a chemical shift reagent into the molecule.[54] Other paramagnetic lanthanides, but not gadolinium, are capable of inducing large chemical shifts. Several studies have been reported on europium, ytterbium, and other lanthanide complexes of DOTA tetraam (DOTAM) derivatives[54,55] (Figure 2.11) that contain two sources of exchangeable hydrogen — the coordinated water and the amide N-H. With the DOTAM ligand, water exchange is so slow that the gadolinium analog is not useful as a T_1 agent. However, the slow water exchange does mean that the $\Delta\omega\tau > 1$ requirement is met.

Water or proton exchange is obviously critical for this class of contrast agents. NMR is an ideal method for measuring this type of exchange. Depending on the rate of exchange, different techniques are used. Line shape analysis of the exchangeable proton can be done if the system is in slow exchange to intermediate exchange. Saturation transfer itself can be used to determine slow exchange rates. When line broadening is not apparent, two-dimensional exchange correlation

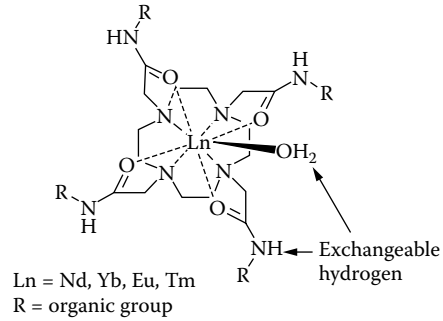

FIGURE 2.11 DOTA tetraamide (DOTAM) derivatives used as PARACEST agents have two sources of exchangeable hydrogen: the N-H amide hydrogen and the hydrogens on the exchangeable water molecule.

spectroscopy (EXSY) is useful. In the case of fast exchange with paramagnetic systems, it is often possible to measure the relaxation rates of the unbound water to determine the exchange rate. Because there is so much water in excess of the paramagnetic ion, the paramagnetic effect on relaxation is diluted. By extrapolating the observed rate to that of a single metal-bound water, estimation of very fast relaxation rates can be made. Varying the temperature or magnetic field is an excellent means of moving the system from slow to fast exchange and enables good estimation of this important parameter. Bertini and Luchinat give an excellent review of relaxation in the presence of chemical exchange.[56]

2.9 DIRECT OBSERVATION OF NONHYDROGEN NUCLEI

The lack of sensitivity in MRI stems from the very small degree of polarization among the nuclear spins. In a magnetic field there is a net magnetization, but this is small; about 0.0006% of the spins are polarized. A technique called spin exchange using a high-powered laser (also called optical pumping) can increase the polarization by four to five orders of magnitude (hyperpolarization).[57] Isotopes possessing long T_1 values can be hyperpolarized and used as contrast agents. The long T_1 is necessary to maintain the contrast medium in the hyperpolarized state long enough to image before the spins relax back to the equilibrium value.

Gases often have long T_1 values, and isotopes of the noble gases helium (^{3}He) and xenon (^{129}Xe) have been used for imaging. Recently, contrast agents with hyperpolarized carbon-13 were reported. Svensson and coworkers[58] described a ^{13}C-enriched water-soluble compound, (bis-1,1-(hydroxymethyl)-1-^{13}C-cyclopropane-d_8), that had long relaxation times (*in vitro*: T_1 = 82 sec, T_2 = 18 sec; *in vivo*: T_1 = 38 sec, T_2 = 1.3 sec). This could be formulated at a ^{13}C concentration of 200 m*M* and hyperpolarized to 15%. The authors used this material for a contrast-enhanced magnetic resonance angiography (CE-MRA) in rats. A major benefit of hyperpolarized contrast media is the excellent sensitivity and no background (high SNR). Challenges include the distribution and availability of the hyperpolarization equipment and imaging hardware compatibility for imaging nonhydrogen nuclei (not available on all clinical scanners).

The fluorine-19 isotope is 100% naturally abundant, and ^{19}F possesses a high magnetogyric ratio, giving ^{19}F a sensitivity that is 83% that of ^{1}H. For other spin = 1/2 nuclei, such as ^{13}C or ^{31}P, the sensitivity is only 0.02 or 6.6% that of the proton. Fluorine imaging has no background since there is very little fluorine in the body. There has been renewed interest in using fluorine as a probe for MRI. Ahrens et al.[59] used perfluorocarbon agents to load dendritic cells and then used ^{19}F MRI to track the cells *in vivo*. The Washington University group have a perfluorocarbon emulsion-based particle as a platform for targeted T_1 agents. Recently this group has demonstrated direct ^{19}F imaging of the particle.[60] Fluorine-containing gases have also been proposed as lung imaging agents.[61,62]